PODOCYTOPENIA IN DIABETIC NEPHROPATHY: A ROLE FOR THE THROMBOXANE A_2 TP RECEPTOR

Gwendoline Carine Denise Bugnot

This thesis has been submitted to the Faculty of Graduate and Postdoctoral Studies as a partial fulfillment to the requirements of the degree of Master in Science program in Cellular and Molecular Medicine.

Department of Cellular and Molecular Medicine

Faculty of Medicine

University of Ottawa

©Gwendoline Carine Denise Bugnot, Ottawa, Canada, 2013

Abstract

Although the etiology of diabetic nephropathy is still uncertain, proteinuria due to podocyte injury and loss (podocytopenia) are early features of the disease. Significant increases in thromboxane A_2 (TXA_2) production as well as expression of its receptor in animal models of diabetic nephropathy led to the hypothesis that TXA_2 acting via its thromboxane-prostanoid (TP) receptor induces podocytopenia resulting in proteinuria.

Systemic infusion of a TP antagonist demonstrated an important role of TXA_2/TP signalling in our model of streptozotocin induced type-1 diabetic nephropathy by reducing kidney damage including proteinuria. Podocyte specific TP overexpressing mice did not demonstrate more pathologic or dynamic kidney damage than non-transgenic mice in STZ-induced diabetic nephropathy. Further assessment of the TP transgene functionality in this mice line is necessary to validate those results.

Whereas the importance of TXA_2/TP signalling is undeniable in diabetic nephropathy, it appears that podocyte TP receptors might not be directly targeted.

Résumé

La néphropathie diabétique est caractérisée par la perte de podocytes induisant la protéinurie, mais son origine reste incertaine. La production de thromboxane A_2 (TXA_2) ainsi que l'expression de son receptor étant significativement augmentée dans différents modèles animaux, nous formons l'hypothèse que le TXA_2 agissant sur son récepteur thromboxane-prostanoides (TP) induit la podocytopénie résultant en protéinurie.

L'infusion systémique d'un antagoniste au récepteur TP démontre un rôle signalétique important de TXA_2/TP en réduisant les dommages rénaux induits par l'injection de streptozotocine. . Les souris surexprimants TP spécifiquement dans les podocytes ne démontrent pas plus de dommages structuraux ou dynamiques que les souris non-transgéniques dans ce modèle. Une évaluation plus approfondie de la fonctionnalité du récepteur transgènic TP dans cette lignée de souris est nécessaire pour valider ces résultats.

L'importance de la signalisation via TXA_2/TP est indéniable dans la néphropathie diabétique, cependant les récepteurs TP des podocytes ne semblent pas être directement impliqués.

Table of contents

List of figures

Chapter I: Introduction

Chapter II: Materials and Methods

Chapter III: Results - Part 1

Chapter III: Results - Part 2

Chapter IV: Discussion

Appendices

List of tables

Chapter II: Materials and Methods

Chapter III: Results - Part 1

Chapter III: Results - Part 2

List of abbreviations

AA	Afferent arteriole
ACVS	Animal care and veterinarian services
a.u.	Arbitrary unit
ACEi	Angiotensin converting enzyme inhibitor
AMDCC	Animal Models of Diabetic Complications Consortium
ARB	Angiotensin receptor blocker
AT_1	Angiotensin-II receptor type 1
BP	Blood pressure
BW	Body weight
C	Capillary
Ca^{2+}	Calcium
CD	Collecting duct
cDNA	Complementary DNA
CKD	Chronic kidney disease
CO_2	Carbon dioxide
COX	Cyclooxygenase
COXIBs	COX-2 inhibitors
Ct	Cycle threshold
d	day
DM	Diabetes Mellitus

DMSO	Dimethyl sulfoxide
DN	Diabetic nephropathy
DNA	Deoxyribonucleic acid
DT	Distal tubule
eGFR	Estimated GFR
EA	Efferent arteriole
ELISA	Enzyme-linked immunosorbent assay
ESRD	End stage renal disease
FBS	Foetal bovine serum
FITC	Fluorescein Isothicyanate-inulin
G	Glomerulus
GBM	Glomerular basement membrane
GFB	Glomerular filtration barrier
GFR	Glomerular filtration rate
HBSS	Hank's buffered salt solution
Hrs, min, s	hours, minutes, seconds
IgG	ImmunoglobulinG
KCl	Potassium chloride
LH	Loop of Henle
µ	micro
MD	Macula densa
mg, ml, mm	milligrams, milliliters, millimeters

mM	millimolar
mmHg	millimeters of Mercury
$MgSO_4$	Magnesium sulfate
mRNA	messenger RNA
Na-Citrate	Sodium Citrate
NaCl	Sodium chloride
NaH_2PO_4	Monosodium phosphate
$NaHCO_3$	Sodium bicarbonate
Nckap5-l	Nck associated protein 5-like
NSAIDs	Non steroidal anti-inflammatory drugs
O_2	dioxygene
OCT	Optimal Cutting Temperature
P	Podocyte
PAS	Periodic acid Schiff
PBS	Phosphate buffer saline
PCR	Polymerase chain reaction
PFA	Paraformaldehyde
PGG_2	Prostaglandin G_2
PGH_2	Prostaglandin H_2
PGE_2	Prostaglandin E_2
PGI_2	Prostacyclin
PGD_2	Prostaglandin D_2

PGF_2	Prostaglandin F_2
PKC	Protein kinase C
PPAR	Peroxisome proliferated-activated receptor
PT	Proximal tubule
qPCR	Quantitative PCR
RAAS	Renin angiotensin aldosterone system
RNA	Ribonucleic acid
RPF	Renal plasma flow
rpm	rotation per minute
RPMI	Roswell park memorial institute medium
SD	Slit diaphragm
S.E.M.	Standard error of the mean
SOD-1	Superoxide dismutase-1
STZ	Streptozotocin
TP	Thromboxane-Prostanoid receptor
TP^{pod+}	Podocyte specific thromboxane receptor overexpressor
TXA_2	Thromboxane A_2
TXB_2	Thromboxane B_2
TXI	Thromboxane synthase inhibitor
TXRA	TP antagonist
U	Ureter
WT-1	Wilm's tumor 1

Acknowledgments

Je souhaite remercier en priorité, ma famille qui m'a soutenue tout au long de mes études aussi bien moralement que financièrement. Bien que des milliers de kilomètres nous séparent, il m'aurait été très difficile d'affronter les épreuves que j'ai rencontré au cours de ces dernières années sans votre soutient.

To my boyfriend David, shall all the obstacles on our way be as easy to go through in the future. Adding to my love, you will always have my sincere gratitude for your kindness and patience.

Apart from moral support, a lot of the work I was able to accomplish during those last two years is partially due to great collaboration with the staff of the animal care and veterinarian services of the University of Ottawa. The professionalism and enthusiasm your team shows represent a pleasant work environment.

I would also like to acknowledge Anthony Carter for his constant help with mice breeding and genotyping as well as his instruction in surgical procedures; Dylan Burger for his training on the live-imaging microscope and his constant availability to answer questions; and finally Chet Holterman for his guidance on PCR reactions and advises regarding the project.

I am grateful to my supervisor, Christopher Kennedy, for believing in my technical skills and overpassing the language barrier. Your constant availability and enthusiasm rendered possible the amelioration of some professional skills that will surely be used in the future.

To Richard Hébert and Mario Tiberi, I appreciated your implication as my advisory committee members; your advice and feed-back were very useful.

Finally I would like to wish the best for the future to the entire kidney research centre members I have met during the last two years.

Chapter I: Introduction

1. Diabetes and diabetic nephropathy

Despite sharing common symptoms (e.g., hyperglycemia and polyuria) and common complications (e.g., cardiovascular disease, neuropathy, retinopathy and nephropathy), the origin of the two classes of diabetes mellitus (DM) vary. Type-2 diabetes, also known as insulin-independent, results from an acquired resistance to insulin by muscle, liver and fat cells, and it occurs mostly in older or obese individuals. On the other hand, type-1 or insulin-dependent diabetes, consists of an autoimmune disorder targeting the insulin producing β-cells of the pancreas. The latter is triggered by environmental factors in genetically predisposed subjects (van Belle, Coppieters *et al.* 2011). The constant increase in environmental triggers, especially in industrialised countries, emphasize the statement of the International Diabetes Federation (IDF) characterizing DM as "one of the most common non-communicable diseases" in the world ((IDF) 2009).

As reported by the 2012 atlas, published by the United States Renal Data System, diabetes accounted for 43.1% of the prevalence of chronic kidney disease (CKD) between the years 1988 and 1994, and for 40.1% between 2005 and 2010 according to the National Health and Nutrition Examination Survey (NHANES). In the same report, it is stated that diabetes remains the leading cause of end-stage renal disease (ESRD) since 1982 reaching more than 50000 new cases in 2010 (System 2012).

Whereas the first link between diabetes and kidney disease dates back to 1936 (Kimmelstiel & Wilson 1936), it is in the 1970's that the description of diabetic nephropathy (DN) progression was outlined. The speed of diabetic nephropathy progression through the five stages of chronic kidney disease varies between patients with an average of 20 years (Figure 1). The first stage is characterized by kidney hypertrophy and hyperfiltration with increased glomerular filtration rate (GFR) and renal plasma flow (RPF); the second stage involves more subtle histological changes, with glomerular hypertrophy, glomerular basement membrane (GBM) thickening and mesangial and tubulointerstitial expansion. The appearance of microalbuminuria with levels between 30 and 200mg/24hrs with an increased likelihood for hypertension defines stage 3. Levels of proteinuria greater than 300mg/24hrs indicate stage 4. A decrease in GFR appears simultaneously with the increase in albuminuria. Stage 5 or end-stage renal disease (ESRD) is declared when GFR is lower than 15ml/min (Kalant 1978; O'Donnell, Kasiske *et al.* 1988; Ayodele, Alebiosu *et al.* 2004; Burgess 2008; Choudhury, Tuncel *et al.* 2010).

Current treatments for diabetic nephropathy are adapted to each stage of disease progression. A constant control of glycemia (mainly by insulin-therapy) as well as control of blood pressure (treatments with renin-angiotensin-aldosterone system (RAAS) blockers: angiotensin converting enzyme inhibitors (ACEi) or angiotensin receptor blockers (ARB)), and limitation of lipid oxidation by statins help to slow diabetic nephropathy progression toward ESRD by reducing the appearance of proteins in urine.

Control of protein intake also appears to be beneficial (Mogensen 1994; Marcantoni, Ortalda *et al.* 1998; Ayodele, Alebiosu *et al.* 2004; Lewis & Lewis 2004; Marshall 2004; Choudhury, Tuncel *et al.* 2010). Despite these interventions, progression toward ESRD cannot be reversed, thereby highlighting the need for novel therapeutic targets and intervention strategies.

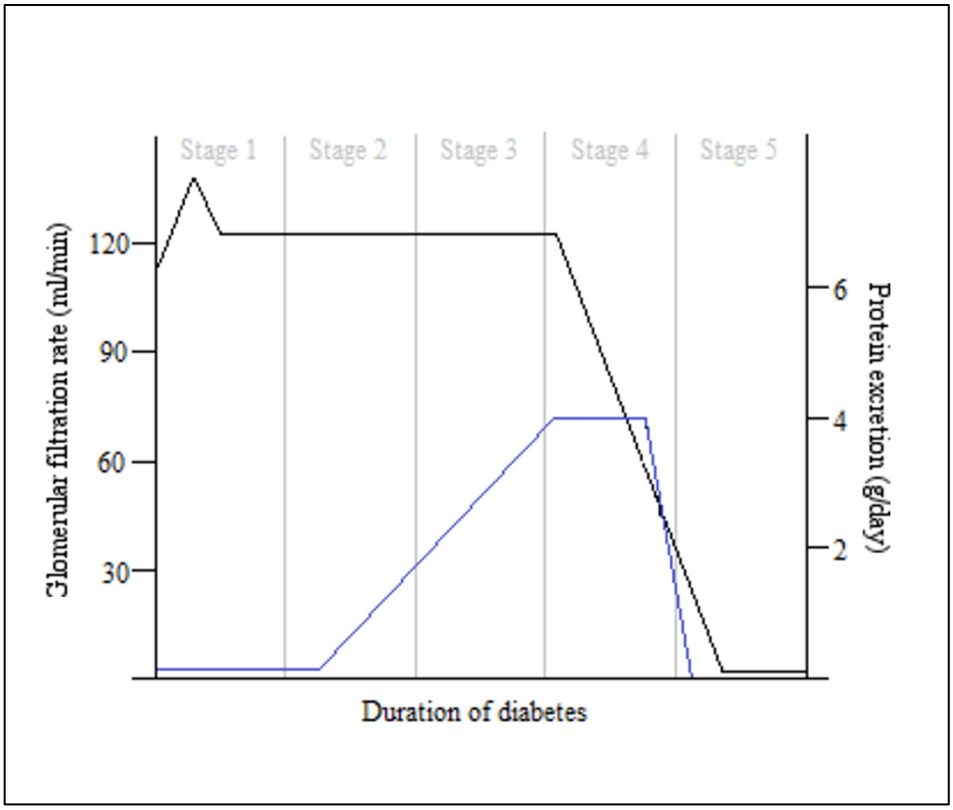

Figure 1: Diabetic nephropathy progression.

This schematic indicates variations of glomerular filtration rate (ml/min) and levels of protein excretion (g/d) through each stage of diabetic nephropathy progression. *Inspired from Burgess, E., 2008* (Burgess 2008).

2. Renal physiology

Kidneys have two major functions: they help to maintain homeostasis by filtering plasma and forming urine and they participate in the regulation of systemic and renal hemodynamic actions by secreting vasodilatory and vasoconstrictory hormones (Helmut G. Rennke & Bradley M. Denker 2007). Glomeruli are recognized as the filtration units of the kidney. A total of 1 million glomeruli in each kidney allow the average filtration of 180 litres of plasma per day. Each glomerulus is connected to a single nephron. Together, these functional units can be divided into five distinct sections: renal corpuscle, proximal convoluted tubule, loop of Henle consisting of descending and ascending limbs, distal convoluted tubule, and collecting duct. The glomerulus is a complex network of capillaries encased by Bowman's capsule and responsible for plasma filtration. After entering the glomerulus through the afferent arteriole, the blood spreads into the capillary network where it is pressed against the glomerular filtration barrier to further merge again and exit the nephron through the efferent arteriole (Figure 2, C.) (Koeppen & Stanton 2007).

The glomerular filtration barrier acts as a sieve and functions as the result of a combination of various components: endothelial glycocalyx, fenestrated endothelial cells, glomerular basement membrane (GBM), differentiated epithelial cells (also named podocytes), and the slit diaphragm (SD). The latter is created by a structural protein based network established between the interdigitations of foot processes from adjacent

podocytes (Figure 2, D.). This highly specialized structure allows free travelling of water and small molecules to form the primary urine into Bowman's space. Molecules larger than 40kDa as well as negatively charged plasma proteins are restricted by the glomerular filtration barrier under physiological conditions (Chang, Deen *et al.* 1975; Chang, Ueki *et al.* 1975; Shankland 2006; Koeppen & Stanton 2007; Menzel & Moeller 2010).

Even if all the layers of the glomerular filtration barrier function together and act interdependently, a growing body of evidence has demonstrated that podocyte injury in particular is linked to increased proteinuria – or leakage of plasma proteins (namely albumin) into urine. Albumin (molecular weight of 67kDa) is a small protein at the limit of sieve's restriction and its appearance in the urine (albuminuria) represents an early indicator of many forms of chronic kidney disease including diabetic nephropathy. Proteinuria can be due to podocyte injury (foot process effacement or detachment) or podocyte loss (detachment or apoptosis) (Pagtalunan, Miller *et al.* 1997; Kriz, Gretz *et al.* 1998; Steffes, Schmidt *et al.* 2001; Susztak, Raff *et al.* 2006; Jefferson, Shankland *et al.* 2008; Jefferson, Shankland *et al.* 2008; Cormack-Aboud, Brinkkoetter *et al.* 2009).
Indeed, Susztak, Raff *et al.* demonstrated that hyperglycemia is a proapoptotic factor on murine podocytes. Their studies showed reduced podocyte numbers per glomerulus associated with the level of albuminuria – which increased with diabetes duration (Susztak, Raff *et al.* 2006).

While the podocyte cell body remains floating in Bowman's space, its primary processes extend and further elaborate into foot processes which wrap around the glomerular basement membrane to establish a large ultra-filtration surface area. This unique cellular shape requires a well-developed actin-based cytoskeleton consisting of the formation of various types of cytoskeleton elements such as microtubules, as well as micro- and intermediate filaments. Actin is the main component of the podocyte's foot processes; linker and adaptor proteins such as myosin and α-actinin-4 are responsible for the network formation within the foot processes and are involved in remodelling post-injury.

The attachment of the foot processes to the glomerular basement membrane involves matrix receptors from the podocyte. The dystroglycan complex links the actin cytoskeleton to some components of the glomerular basement membrane whereas integrins, some transmembrane molecules characteristic of each cell type, form an heterodimer between the α3 chain of the collagen IV of the basement membrane and the β1 integrin subunit in the foot processes.

As mentioned earlier, interdigitations of podocytes foot processes allow formation of the slit-diaphragm. Nephrin is the main component of the slit-diaphragm and is anchored to each podocyte foot process by ZO-1, podocin, and CD2-associated protein. The resulting protein complex bridges the gap between adjacent foot processes to form a filtration slit pore that effectively restricts the passage of macromolecules such as albumin while allowing for a free flow of water and electrolytes.

In diabetes, hyperfiltration associated with increased glomerular capillary pressure exposes podocytes to mechanical stress due to capillary wall distension, leading to cytoskeletal reorganization, loss of slit diaphragm integrity and loss of integrin expression, resulting in proteinuria (Pavenstadt, Kriz *et al.* 2003). The link between podocyte detachment and integrin expression has been demonstrated by Regoli and Bendayan. In their study, hyperglycemic rats have a lower expression of subunit α3 from integrin α3β1 in podocytes (Regoli & Bendayan 1997). This discovery was later confirmed by Chen, Chen *et al.* who quantified a reduced glomerular integrin expression in STZ-induced type-1 DM in rats. They also confirmed reduced expression of integrin in kidneys of diabetic patients compared with non diabetic patients (Chen, Chen *et al.* 2000).

From these studies, it appears that podocyte apoptosis and/or detachment are the main cause of proteinuria in diabetic nephropathy. However, the identity of each of the factors implicated in this destructive process remains incomplete.

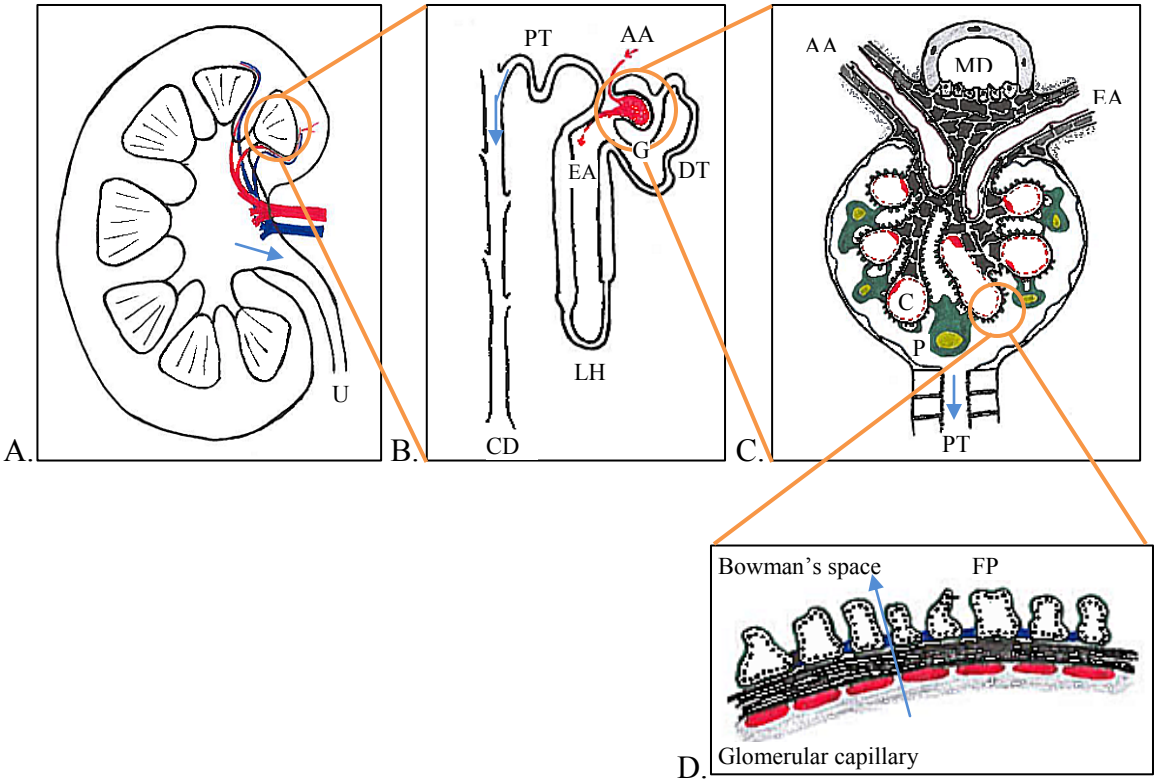

Figure 2: Schematic representations of the kidney, nephron, glomerulus, and filtration barrier.

Schematic representation of a longitudinal cut of a kidney (A), a nephron (B), a glomerulus (C) and the glomerular filtration barrier (D). The blue arrow indicates the direction of the filtration and urine collection. Renal artery, renal vein (red and blue in picture A); slit diaphragm, glomerular basement membrane, fenestrated endothelial cells, glycocalyx (blue, black, red, grey in picture D) ; AA: Afferent Arteriole, C: Capillary, CD: Collecting Duct, DT: Distal Tubule, EA: Efferent Arteriole, FP: Foot Processes, G: Glomerulus, LH: Loop of Henle, MD: Macula Densa, P: Podocyte, PT: Proximal Tubule, U: Ureter

3. Arachidonic acid pathway and GFB damage

The involvement of cyclooxygenase-2 (COX-2) in proteinuria is due to its enzymatic action on arachidonic acid. The latter is released from the cellular membrane by the action of the phospholipase A_2.

A number of studies have demonstrated a role for a class of lipid based mediators, termed prostanoids, in the etiology of albuminuria. The prostanoids are derived from the enzymatic actions of cyclooxygenases. Those enzymes transform arachidonic acid in endoperoxids, prostaglandin G_2 (PGG_2), and further prostaglandin H_2 (PGH_2). PGH_2 is the common substrate of thromboxane and prostanoids synthases. Each product (PGE_2, PGI_2, PGD_2, PGF_2 and thromboxane $A_{2)}$ acts on a specific cell surface G-coupled receptor (Figure 3).

Two isoforms of cyclooxygenase have been identified. Cyclooxygenase-1 (COX-1) has been known as the housekeeping enzyme responsible for a variety of global physiological responses (mucosa protection, platelet aggregation, and renal blood flow). In contrast, COX-2 has been postulated as the pathological responder, mainly expressed in inflammatory cells. COXs isoforms share 60% homology in the amino acid sequence. COX-2 contains 18 additional amino acids at the C-terminal location. The change in 434 and 523 residues (isoleucine in COX-1 and valine in COX-2) plays an important role in the selectivity to COX-2 inhibitors in the hydrophobic region of the COXs sequence. In

fact, variation in size between the two residues allows creation of a larger pocket which could influence COX-2 inhibitors binding (Hinz & Brune 2002; Warner & Mitchell 2004).

Despite identical enzymatic properties, both isoforms display divergent expression patterns throughout the kidney. COX-1 immunoreactivity was detected in the collecting duct, thin loop of Henle, some parts of the vasculature, and in glomeruli; whereas COX-2 was detected in the macula densa, medullary interstitial cells, the vasculature, and human podocytes (Komers, Lindsley *et al.* 2001; Hinz & Brune 2002; Warner & Mitchell 2004).

In 1971, it was hypothesized that inhibition of COXs would result in reduction in pro-inflammatory prostaglandins. Therefore, non steroidal anti-inflammatory drugs (NSAIDs) such as ibuprofen or salicylic acid based compound, for instance aspirin, were used for their anti-inflammatory, analgesic and antipyretic effects. Unfortunately, those drugs presented some side effects such as gastrointestinal ulceration and platelet dysfunction. These unwanted side effects were attributed to the actions on COX-1 housekeeping enzyme. Pharmaceutical development of COX-2 inhibitors (Coxibs) helped to diminish the side effects previously mentioned while preserving positive effects (FitzGerald & Patrono 2001; Hinz & Brune 2002; Simmons 2003; Warner & Mitchell 2004; Nasrallah, Clark *et al.* 2007).

Animal studies using COX-2 inhibitors appeared promising with decreased proteinuria, and clinical trials presented reduction in ulcers generation (Vriesendorp, Donker *et al.* 1986). However, several Coxibs (e.g., Rofecoxib) had to be withdrawn from clinical use due to a significant increase in cardiovascular risks. The hypothesis of an unbalanced ratio between some of downstream COX effectors (PGI_2 and TXA_2) due to selective inhibition may account for these effects (Zatz & Fujihara 2002; Fitzgerald 2004; Warner & Mitchell 2004).

A large number of studies have demonstrated enhanced COX-2 expression in kidney diseases. In fact, a model of type-1 diabetes increased COX-2 expression in the renal cortical region of rats (Komers, Lindsley *et al.* 2001). When mouse podocytes were exposed to mechanical stretch, recreating the impact of increased glomerular capillary pressure, COX-2 mRNA and protein expression were elevated (Martineau, McVeigh *et al.* 2004). In order to assess the role of COX-2 in filtration barrier dysfunction in chronic kidney disease, inhibitory studies were carried out in animal models. Specific inhibition of COX-2 had a renoprotective effect in rats subjected to renal mass reduction (partial nephrectomy) by partially preventing proteinuria and preserving glomerular and tubular structure (Wang, Cheng *et al.* 2000). Additionally, podocyte specific COX-2 overexpressor mice were protected against foot processes effacement and proteinuria observed in the model of minimal change disease when administrated a COX-2 inhibitor (Cheng, Wang *et al.* 2007). These studies along with many others support the notion that glomerular COX activity leads to filtration barrier damage in disease settings. However,

the downstream prostanoid receptor(s) as well as their cellular locales that mediate these deleterious effects remain to be identified.

Moreover, COXs are the source of a wide range of prostanoids: prostacyclin (PGI_2), PGE_2, PGF_2, PGD_2, and thromboxane A_2 (TXA_2). Inhibiting the production of such diversity of molecules may lead to an imbalance in cellular mechanisms resulting in unwanted side effects. Since current treatments allow only a partial reduction in proteinuria, it is important to identify specific downstream targets detrimental to the glomerular filtration barrier, in order to generate fewer side effects while simultaneously preventing progression toward ESRD.

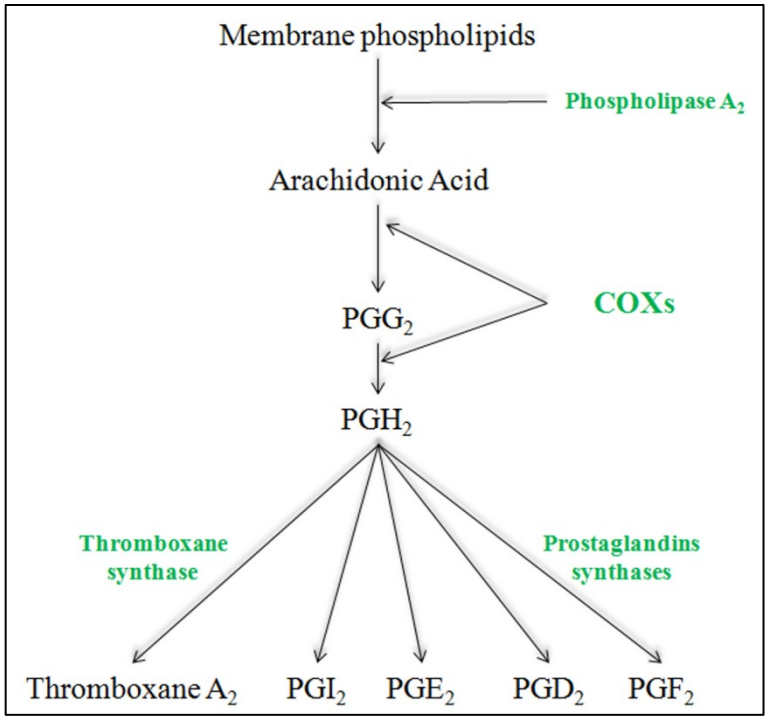

Figure 3: Prostaglandins and thromboxane synthesis, the arachidonic acid pathway.

Arachidonic acid derived from membrane phospholipids is enzymatically transformed into PGH_2 by either isoform of cyclooxygenase (COX-1 or COX-2). Various prostaglandins synthases or thromboxane synthase give final products or signal messengers. *Inspired from* (Cathcart, Reynolds *et al.* 2010)

4. Thromboxane A_2 and the TP receptor

A growing body of evidence suggests that TXA_2 and its thromboxane-prostanoid (TP) receptor are reasonable targets for diabetic nephropathy therapy. Cheng, Fan *et al.,* demonstrated that the TP receptor mRNA levels and its ligand (TXA_2) are upregulated in podocytes heterologously overexpressing COX-2. They also linked thromboxane A_2 production with increased proteinuria, podocytes apoptosis, and foot processes effacement in a mouse model of adriamycin nephropathy. These were largely prevented by either treatment with a TP receptor antagonist or in mice with global deletion of the TP receptor (Cheng, Fan *et al.* 2009). Although these findings suggest a role for the TP receptor in mediating filtration barrier damage in chronic kidney disease, other studies have examined its role in models of diabetes. For example, treatment with both thromboxane synthase inhibitor (TXI) and TP receptor antagonist (TXRA) in type-1 diabetic rats decreased albuminuria and yielded a lower production of thromboxane A_2 metabolite: thromboxane B_2 (TXB_2) (Craven, Melhem *et al.* 1992). In the STZ-induced diabetic mouse model, the thromboxane A_2 antagonist S18886 reduced proteinuria significantly compared to NSAIDs (Xu, Jiang *et al.* 2006). The same molecule administered to type-2 diabetic rats protected kidney function, decreased proteinuria, and resulted in less histomorphological damage (Sebekova, Eifert *et al.* 2007).

These studies implicate the thromboxane A_2/TP receptor in glomerular filtration barrier injuries in diabetic nephropathy. However, whether the podocyte is the site of TXA_2/TP receptor actions remains to be determined.

As discussed earlier, thromboxane A_2 is derived from arachidonic acid. It has a short half-life (30s), so that its actions are carried out in an auto or paracrine signalling manner. Non enzymatic transformation of the thromboxane A_2 into the inactive metabolite, thromboxane B_2, was first detected in the platelet (Hamberg, Svensson *et al.* 1975). Since then, many organs and cells have been identified as sites of thromboxane A_2 production with lungs, spleen, liver, and leukocytes presenting the highest mRNA expression of thromboxane synthase (TXS) (Cathcart, Reynolds *et al.* 2010). TP receptor is expressed in the heart, kidney, uterus, and vascular cells where thromboxane A_2 is generated (Woodward, Jones *et al.*; Woodward, Jones *et al.* 2011). In the podocyte, mRNA expression of TP receptor has been shown (Bek, Nusing *et al.* 1999).

The TP receptor is present in two different isoforms in humans (TPα and TPβ). Both isoforms issue from the same gene on chromosome 19. Differences found in their C-terminal region does not affect their functionality toward their ligand but induce a variation in their subcellular location. In their study, Fanelli, Mauri *et al.,* showed that TPα remains localized at the cell membrane whereas TPβ gets internalized after TP agonist stimulation. They also demonstrated that the TPα/TPβ heterodimer is able to internalize, leading to the hypothesis that TPβ is responsible for the desensitisation of TP

signalling (Nakahata 2008; Fanelli, Mauri *et al.* 2011). This hypothesis would explain the divergence in mRNA expression in favour of TPα isoform in most tissues (Miggin & Kinsella 1998). This phenomenon is not present in the mouse. In fact the only isoform found in the mouse is 76% homologous with the human TPα sequence. Whereas the ligand binding site remains identical between species, the G-protein coupling sites located on the C-terminal section vary (Nakahata 2008). Mouse-TP desensitization involves phosphorylation of some of the C-terminal serines (Spurney 1998).

Vasoconstriction, bronchoconstriction, and promotion of platelet aggregation are the main known effects of TXA_2/TP signalling. The TP receptor couples mainly to $G\alpha_q$ and $G\alpha_{12/13}$ (Zhang, Brass *et al.* 2009). Other interactions with $G\alpha_i$, $G\alpha_s$, and $G\alpha_h$, have been shown and appear to be tissue or cell dependent. TP coupled $G\alpha_q$ signalling induces Ca^{2+} influx and PKC activation (Figure 4). An increase in intracellular Ca^{2+} in podocytes leads to calcineurin activation, inducing synaptopodin cleavage, and resulting in glomerular filtration barrier damage and proteinuria (Greka & Mundel 2012). In contrast, $G\alpha_{12/13}$ signalling involves RhoA effector (Figure 4). It is hypothesized that synaptopodin stabilizes and protects RhoA against degradation to help to maintain podocyte cytoskeletal architecture. However, aberrantly high RhoA activities have been demonstrated to be injurious for the glomerular filtration barrier (Nakahata 2008; Greka & Mundel 2012).

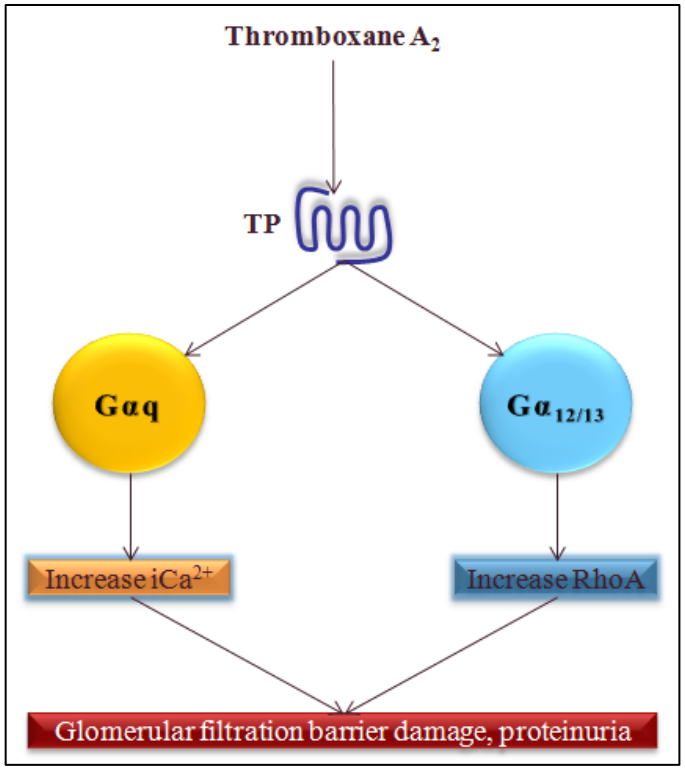

Figure 4: Thromboxane-Prostanoid receptor signalling.

Stimulation of TP receptor by its ligand allows interaction with $G_{\alpha q}$ subunit leading to increased intracellular calcium or with $G_{\alpha 12/13}$ subunit increasing RhoA formation. Both pathway damage the glomerular filtration barrier by triggering podocyte foot process effacement, apoptosis etc – leading to proteinuria.

Rationale

The renoprotective effects of TP receptor antagonist administration have been demonstrated in various models of kidney disease (Craven, Melhem *et al.* 1992; Xu, Jiang *et al.* 2006). Studies of type-2 diabetes mouse models and a type-1 diabetes rat model showed that the blockade of TXA_2/TP signalling prevents or delays glomerular filtration barrier damage. However, no studies have yet examined a role for the TXA_2/TP receptor in mediating glomerular injury in type-1 diabetic mice.

The expression of TP receptor at the cellular membrane of podocytes as well as the discovery of a renoprotective effect of global TP receptor deletion in mice with podocyte-specific COX-2 overexpression is consistent with the notion that the TP receptor is involved in glomerular filtration damages through its actions on the podocyte. Moreover, treatment of mouse podocyte, exposed to puromycin (induction of minimal change disease in rodent models), with a TP receptor antagonist protected the cells against apoptosis (Cheng, Fan *et al.* 2009). However, a more specific link between podocyte loss in diabetic nephropathy and TXA_2/TP signalling still remains to be demonstrated.

Previous work in our laboratory showed increased podocyte apoptosis *in vitro* after stimulation with TP receptor agonist U46619 as well as increased TP receptor mRNA expression in mouse podocytes exposed to diabetic conditions (e.g., high concentrations

of glucose and cyclic mechanical stretch). Taken together these findings allowed us to formulate the following hypothesis:

Hypothesis

Thromboxane A2 acting through its TP receptor expressed on podocytes contributes to glomerular filtration barrier damage and albuminuria in a model of type-1 diabetic nephropathy (Figure 5).

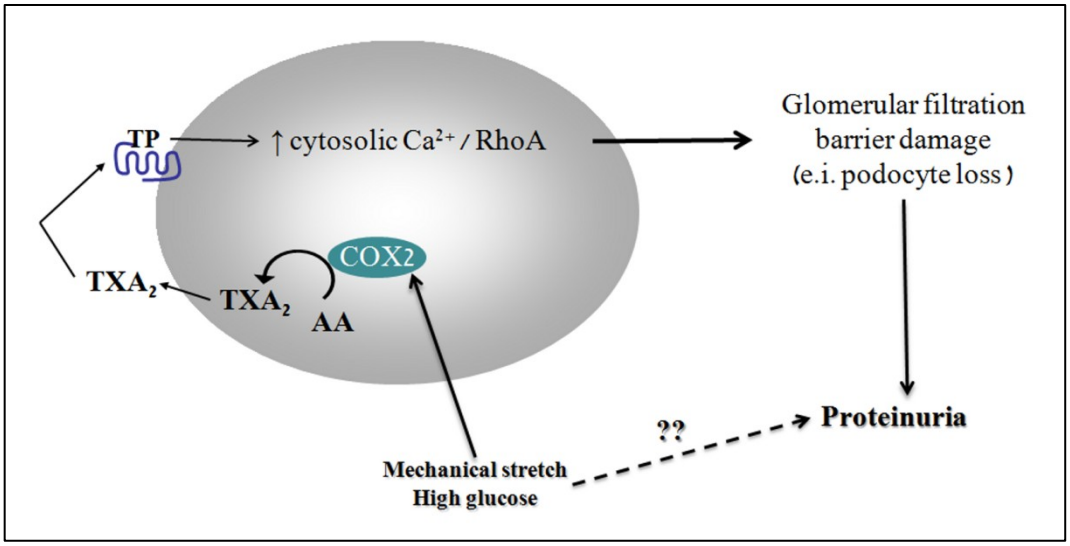

Figure 5: Schematic representation of the hypothesis.

Diabetic conditions (i.e., mechanical stretch and high glucose) stimulate thromboxane A_2 production by increasing COX-2 activity. Acting in an autocrine manner, thromboxane A_2 activates TP receptors at the cell membrane of the podocyte. Elevated intracellular calcium and increased RhoA activity lead to albuminuria by inducing glomerular filtration damage (i.e., podocyte loss).

Objectives

Objective 1: Demonstrate that the TP receptor contributes to albuminuria in diabetic nephropathy. We will show this involvement by administering the TP antagonist SQ29548 to mice with STZ-induced type-1 diabetic glomerular filtration barrier injury.

Objective 2: Test whether podocyte TP receptors underlie the actions of the TXA_2/TP receptor axis on filtration barrier injury in a model of diabetic nephropathy. For this purpose, mice with transgenic overexpression of the TP receptor in podocytes will be characterized and subjected to the STZ type-1 diabetes model and the effects on filtration barrier injury determined.

Relevance

Non steroidal anti-inflammatory drugs (NSAIDs) and COX-2 inhibitors (COXIBs) are known to decrease proteinuria in patients with diabetic nephropathy. However, side effects on the gastrointestinal tract and the cardiovascular system limit their use in patients.

Inhibition of COX-2 leads to a reduction of a broad number of lipid mediators (i.e., prostanoids) suppressing both detrimental and protective effects of those effectors on the vasculature, kidney, and gastrointestinal tract. Identification of detrimental effectors favouring diabetic nephropathy development would allow discovery of more specific pharmaceutical targets, potentially avoiding important side effects. These studies have the potential to improve treatment of patients with diabetic nephropathy with the goal of slowing down or suppressing the progression toward end stage renal disease.

Chapter II: Materials and Methods

1. Characterization of the TP^{pod+} transgenic mice.

Procedures were approved beforehand by the University of Ottawa Animal Care Committee. Isoflurane-induced anesthesia supported all surgical procedures in FVB/n and TP^{pod+} males between 8-10 weeks old.

Genotyping

PCR using primers (Table 1: CKNE11 and TPr) complementary to portions of *NSPH1*-TP transgene was performed on DNA extracted from 3 week old pup tail or ear samples. PCR products were visualized by electrophoresis on a 1.5% agarose gel. By concern for standardization, Anthony Carter was responsible for all mice line genotyping.

Glomerular isolation

Microbeads from 200µl of DynaBeads M-450 Tosylactivated (Invitrogen Dynal AS, Oslo, Norway) suspension were rinsed three times in PBS 1X and collected with a magnetic particle concentrator Dynal MPC-S (Dynal A.S, Oslo, Norway) before being resuspended in 20ml of PBS 1X. The resuspended beads were used to perfuse a single mouse by injection through the left ventricle of the heart, while the excess of perfusate was allowed to escape through an incision in the right atrium. Both kidneys were collected, decapsulated, minced, and added to a digestion solution containing 1mg/ml collagenase, 0.1mg/ml DNase I for 40 minutes with incubation at 37ºC in a water-bath. The digested suspension was pushed through a 100µm sterile cell strainer (Fisher Scientific) pre-

washed by 5ml of HBSS (Multicell, Wisent Inc.). This step was repeated before centrifugation at 1000rpm for 10min. Most of the supernatant was removed and the pellet was resuspended in a small volume of liquid remaining before being transferred to an eppendorf for magnetic collection of the beads. Four to five washes of 600µl PBS 1X each were necessary to obtain a minimal purity of 95% as determined under light microscopy. Glomeruli were resuspended in a small volume of PBS 1X and processed for intracellular calcium measurement or TP agonist U46619 stimulation before RNA extraction.

Intracellular calcium measurement

Freshly extracted glomeruli were seeded on collagen I coated coverslip (part of POC cell cultivation system, Zeiss) contained in a 60mm cell culture dish (BD Falcon, Franklin Lakes, NJ). Culture in RPMI (Invitrogen) 0.5% FBS (ThermoScientific, Hyclone Laboratory, Inc., UT) with 5µM indomethacin (Sigma-Aldrich) for 48 hours in a 37ºC incubator 95:5 air:CO_2 (V:V).

After 48 hours podocytes exhibited growth out of the glomerulus extending onto the coverslip. Media was removed and replaced by calcium measurement buffer (NaCl 120mM, KCl 5.4mM, $MgSO_4$ 1.2mM, NaH_2PO_4 1.2mM, $NaHCO_3$ 20mM, Glucose 5.6mM, pH 7.4). Fura-2AM (Invitrogen) was added to a final concentration of 1µM and incubated for an additional 30 minutes.

Each coverslip was carefully removed from the buffer and mounted on a live-imaging microscope apparatus (Stallion High Speed Digital Microscopy Workstation, Zeiss,

Germany). 450µl of buffer were added to the chamber before starting measurements. Once a baseline of calcium/dye re-activity was established, TP agonist U46619 was added to the media to a final concentration of 1µM. If no signal was detected within the next 15 - 20mins, calcium ionophore A23187 (Sigma-Aldrich) was added to the media to a final concentration of 2µM. If a TP-induced signal was detected, calcium ionophore was added once the signal went back or close to baseline.

Slidebook 4.1 software (Intelligent Imaging Innovations, Inc.) allowed generation of movies out of all the pictures taken as well as a graph presenting the ratio 340nm/380nm of each region selected and analyzed.

TP agonist U46619 stimulation of glomerular extract

Extracted glomeruli were seeded onto 60mm dishes and cultured in the same media described above with addition of TP agonist U46619 at a final concentration of 1µM or with the same volume of methyl acetate as vehicle (Sigma-Aldrich). Incubation lasted 2 hours at 37ºC before glomeruli/cells were collected, resuspended, and centrifuged for 2min at 10000rpm.

RNA extraction, Reverse transcription and quantitative PCR

Approximately 20mg of frozen kidney cortex was crushed using the TP-103 Amalgamator COE Capmixer (GC America, Inc., Alsip, IL): capsules and ceramic beads were dipped into liquid nitrogen prior to frozen sample addition. Once sealed, the capsule was shaken for 10s before the bead was removed. RNA was extracted out of the powder

or out of glomerular extract using an RNeasy Mini-kit (Qiagen) starting with 600µl of RLT buffer.

High-Capacity cDNA Reverse Transcription kit (Applied Biosystems) was used as per manufacturer recommendations to obtain cDNA from 1µg of extracted RNA. Samples were diluted 1:1 with the 2X RT master mix and submitted to reverse transcription cycle (25°C for 10min, 37°C for 120min and 85°C for 5 min) prior to storage.

mRNA expression levels of COX-2, Nckap5-l, Nephrin, Podocin, Sod-1, and total-TP were assessed and normalized to β-actin levels by quantitative PCR using SYBR Advantage qPCR Premix (Clontech Laboratories Inc., Mountain View, CA), 0.8ml optical tubes and caps (Applied Biosystems) and the ABI Prism 7000 Sequence Detection System according to manufacturer instructions. qPCR machine was programmed as described in Table 2. Normalized levels (dCt) of each sample were normalized to the average of non-stimulated/vehicle-injected samples (ddCt) before calculation of relative change (formula: 2^{-ddCt}) allowing appreciation of variations even in the controls and statistical analysis by GraphPad software. Table 1 illustrates all the primers sequences.

Table 1: Primer sequences.

List of primers used for genotyping and quantitative real time PCR displayed in 5' to 3' direction.

Name	Direction	Sequence (5'-3' direction)
CKNE11 (Nphs1 promoter)	Forward	gagaaagaactgttaacggg
TPr	Reverse	acgtcgctcctgcagcgtga
β-actin	Forward	agccatgtacgtagccatcc
	Reverse	tttgatgtcacgcacgattt
COX-2	Forward	agagccggcttggcatccgt
	Reverse	ccgccttgcgacacgaccct
Nckap5l	Forward	gcgcttgcgcaggccaatga
	Reverse	tggggctggggaggttggtcg
Nephrin	Forward	aagctggacgtgcattatgct
	Reverse	cggtgcagactatatccacagaac
Podocin	Forward	catgaagcgcctcttggcac
	Reverse	tggcctgtctttgtgcctca
Sod-1	Forward	agagccggcttggcatccgt
	Reverse	ccgccttgcgacacgaccct
Total TP	Forward	cctcccctcaaccaacgtga
	Reverse	ctgattccagcgcacttggc

Table 2: Quantitative PCR protocol.

Two µl of cDNA, obtained after reverse transcription of 1µg of RNA sample, were added to the SYBR Advantage qPCR Premix following manufacturer instructions. Triplicates of each sample were submitted to a step of denaturation (step 1), a step of 40 cycles of amplification (step 2) and a reaction specificity control (step 3).

Step	**# of cycles**	**Temperature (ºC)**	**Time (s)**
Step 1	1	95	20
Step 2	40	95	20
		60	20
		72	30
Step 3 (dissociation step)	1	95	15
		60	20
		95	15

2. Animal models of diabetic nephropathy

STZ injections

Mice were injected over 5 consecutive days with fresh solutions of 0.1M Na-Citrate pH4.5 (vehicle), 5mg/ml, or 7.5mg/ml of Streptozotocin (STZ, Sigma-Aldrich) diluted in the vehicle solution of Na-Citrate. Injections of 0.1ml/10gBW were done by the Animal Care and Veterinary Service staff. Both doses of STZ: 50 and 75mg/kg are considered low-dose, but throughout this thesis the dose of 50mg/kg will be referred as "low dose" whereas the 75mg/kg dose will be referred as "medium dose". Figure 6 illustrates the experimental design and the timeline of data and sample collection.

Osmotic micro-pumps implantation

Alzet micro-osmotic pumps (Durect Corporation, Cupertino, CA) were implanted subcutaneously in FVB/n males (ordered from Charles River) for chronic delivery of the TP antagonist, SQ29548 (Cayman Chemical, Ann Arbor, MI), simultaneously with STZ injection. SQ29548 was dissolved in 100%DMSO and diluted 1:1 in ddH_2O. Pumps were loaded with the SQ29548 solution or the vehicle solution of 1:1 DMSO:ddH_2O to deliver a constant rate of 660µg/kg/day over 4 weeks. The experimental idea was inspired by the work of Shineman, Zhang *et al.* (Shineman, Zhang *et al.* 2008). Figure 7 is an adaptation of Figure 6 and illustrates the experimental design and the timeline of data and sample collection.

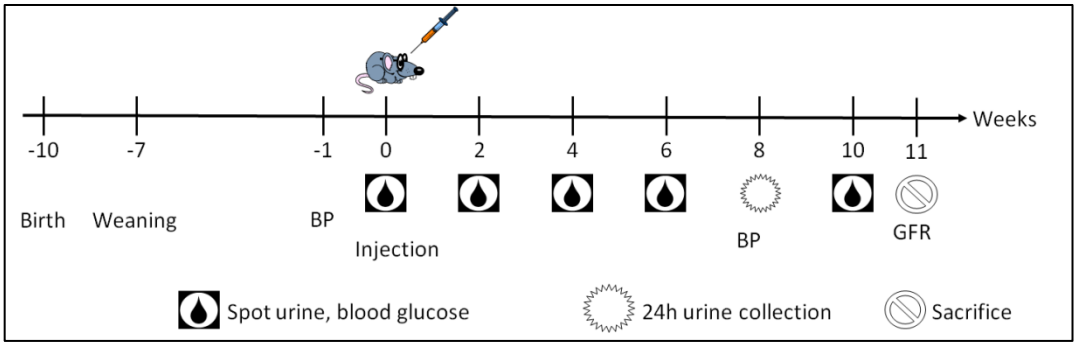

Figure 6: Timeline of the induced type-1 diabetic nephropathy.

Ten week old TP^{pod+} male were injected with 75mg/kg/day or 50mg/kg/day of Streptozotocin (STZ) for five days after measurement of the baseline blood pressure (BP) and blood glucose. Blood glucose levels were determined along with spot urine collections taken biweekly over eleven weeks. Twenty four hour urine collection and blood pressure measurement were scheduled at weeks 8 post-injection. At the end of the study, after determination of the estimated glomerular filtration rate (eGFR) mice were sacrificed, their kidneys were weighed before being split for pathology analysis (4% Paraformaldehyde), frozen section preparation (OCT), electron microscopy (2.4% glutaraldehyde) and protein/RNA analysis (snap frozen in liquid nitrogen).

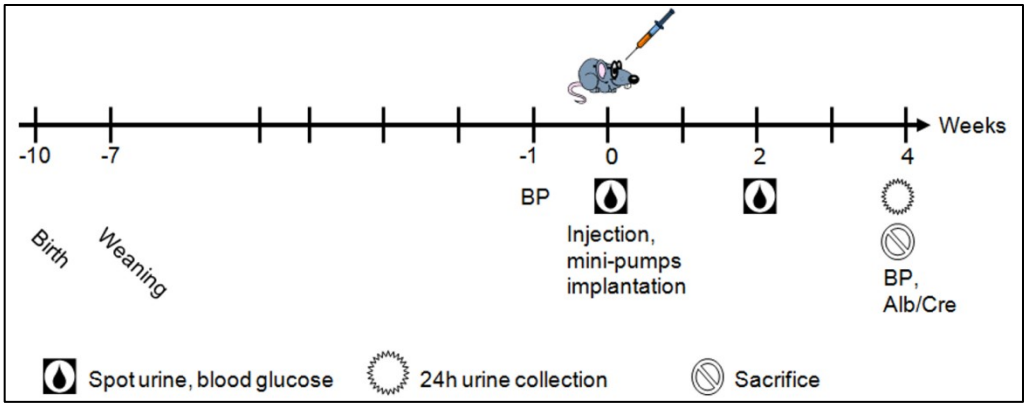

Figure 7: Timeline of the TP receptor antagonist SQ29548 in vivo study.

Ten weeks old non-transgenic males injected with 50mg/kg/day of Streptozotocin (STZ) for five days were simultaneously implanted with osmotic pumps delivering 660µg/kg/day of SQ29548 (1:1 H_2O:DMSO). Blood pressure (BP) was measured at -1 and 4 weeks; blood glucose was measured at -1, 2 and 4 weeks, and spot urine were collected at -1 and 2 weeks post-injection. Twenty four hour urine collection was scheduled at week 4 post-injection to help confirming kidney damages before sacrificing the mice as previously described.

Blood pressure measurements

Tail-cuff plethysmography (BP-2000; Visitech Systems, Apex, NC) was used to measure systolic blood pressure. Five days of training were performed prior to 5 days of data collection. Each session consisted in 5 non-recorded and 10 recorded measures. Blood pressure was assessed prior to STZ injections and at 4 weeks (SQ29548 study) or 8 weeks post-injection (diabetic nephropathy study).

Urinalysis

Twenty four hour urine samples were collected at 4 weeks (SQ29548 study) or at 8 weeks (diabetic nephropathy study) post-injection to measure volume and analyze albumin and creatinine levels using the Mouse Albumin ELISA Kit (Bethyl Laboratories, Inc., www.bethyl.com) and Creatinine Companion Kit (Exocell, Inc., Philadelphia, PA), respectively. To obtain 24 hour collections, mice were housed o/n in metabolic cages and had free access to food and water. Urine was collected in a cylinder located under the wire floor of the cage.

Urine samples were diluted 1:1000 for non-diabetic mice and 1:2000 for diabetic mice for the albumin kit. Dilution of samples for the creatinine kit were 1:20 for non-diabetic mice whereas diabetic urine samples were tested undiluted.

Albuminuria was normalized to either creatinine level (µg/mg) or to 24hrs volume (µg/24hrs).

Blood glucose quantification

Plasma samples were processed by centrifugation (13000rpm, 20min, 4ºC) of cardiac puncture blood samples obtained at the end of the experimental period. Aliquots of plasma were sent to IDEXX Laboratories, Inc. (Markham, ON) or using the OneTouch Ultra2 glucometer (Lifescan Inc., Milpitas, CA) to determine glucose concentration.

Glomerular filtration rate

Estimation of the glomerular filtration rate was assessed following a single tail-vein injection of Fluorescein Isothicyanate-inulin (FITC-inulin) according to Animal Models of Diabetic Complications Consortium (AMDCC). The solution of 5% FITC-inulin (Sigma-Aldrich) dissolved in 0.9% NaCl, dialysed overnight, and sterilised was injected at a dose of 3.74µl/gBW in isoflurane anesthetized mice. Blood was collected from the saphenous vein in heparinised capillary tubes (Fisher Scientific) at 3, 7, 10, 15, 35, 55, and 75 minutes post-injection. Samples were assayed as described in the AMDCC protocol. A two-compartment clearance model was employed in GraphPad Prism 5.02 software to calculate GFR values expressed as ml/min.

Renal pathology

Isoflurane anesthetized mice were perfused with 20ml of ice-cold PBS through the left ventricle. Clearing of the circulatory system necessitated a small cut in the right atrium. Poles of each kidney were removed after extraction and decapsulation. Portions of kidneys were placed either in 4% paraformaldehyde (PFA)/PBS for paraffin embedding

or embedded in O.C.T. (Optimal Cutting Temperature) Compound (Sakura Finetek USA Inc., Torrance, CA) for frozen sectioning. 4µm sections stained with periodic acid Schiff (PAS) were analyzed by light microscopy using a Zeiss AxioCam microcope (Zeiss Axio Imager.A1, Zeiss Germany). Glomerular area (glomerular tuft and urinary space of Bowman's capsule) from 20 glomeruli per mouse was measured using Axiovision Rel 4.8 software.

Immunofluorescence, WT1 staining

Optimal cuttingtemperature media (O.C.T.) embedded frozen tissue samples were serially cut in 8µm sections. Slides were allowed to heat to ambient temperature for an hour prior to being fixed for 10min in ice cold acetone and air dried for 30min. Sections were then rehydrated for 15min in PBS 1X, blocked for 30min in PBS 1X, 0.1% Bovine Serum Albumin (BSA, Sigma-Aldrich), 10% Donkey serum (Jackson) and incubated for 1hour with PBS 1X, 0.1% BSA, 2% Donkey serum with or without mouse polyclonal anti-WT1 (Wilm's tumor protein, SantaCruz, Santa Cruz, CA; dilution 1:200). After three washes of 5min each in PBS 1X, sections were incubated for 45min with the same solution described above with donkey anti-rabbit IgG Alexa Fluor 488 conjugated (Invitrogen, Molecular probes, Eugene, OR; dilution 1:500). Images were captured using a Zeiss AxioCam microscope and the analysis of 20 glomeruli per mouse was performed using Zeiss Axiovision Rel 4.8 software.

Statistical analysis

Two-way ANOVA or one-way ANOVA with Bonferroni post test was performed on all experimental data using GraphPad Prism version 5.02 for windows, GraphPad Software, San Diego California USA, www.graphpad.com. Graphs indicate values with standard error of the mean (S.E.M.). Differences between groups were considered statistically significant if $p<0.05$.

Chapter III: Results

Part 1: Administration of a thromboxane receptor antagonist to mice with streptozotocin-induced diabetes.

Rationale

A number of studies have employed various TP antagonists in rodent models of chronic kidney disease (Craven, Melhem *et al.* 1992; Xu, Jiang *et al.* 2006; Sebekova, Eifert *et al.* 2007). In general, TP antagonism reduces indications of renal injury, including albuminuria, suggesting that the thromboxane, acting via its cell surface TP receptor, activates intracellular signalling pathways that contribute either directly or indirectly to glomerular filtration barrier damage. Although studies involving administration of TP antagonists have been carried out in diabetic rats, no such work has been reported in mouse models. We therefore set out to test the hypothesis that *in vivo* TP antagonism in STZ-induced diabetic mice would attenuate albuminuria and glomerular injury.

Confirmation of type-1 diabetes

To address this hypothesis, 10 week old FVB/n males were injected with either STZ (50mg/kg/day) or Na-Citrate vehicle and implanted with mini-pumps diffusing 660µl/kg/day of TP antagonist SQ29548 or 330µl/kg/day of 50%DMSO vehicle. FVB/n mice were chosen as this strain exhibits a relatively robust susceptibility to filtration barrier damage in response to STZ-induced diabetes (Xu, Huang *et al.* 2010). Furthermore, male mice are more susceptible to diabetic injury than female mice.

At 4 weeks post-injection, mice were sacrificed and plasma glucose levels were measured ; values are reported in Table 3. There was significantly increased glycemia in the STZ-injected mice (29.0 ± 2.1mM [*n*=6] for vehicle infused mice and 26.7 ± 2.3mM [*n*=6] for SQ29548 infused mice) compared to the respective non-diabetic controls (18.5 ± 0.9mM, $p<0.001$ [*n*=5] and 18.0 ± 0.9mM, $p<0.01$ [*n*=6]). This finding, indicates a successful effect of the toxin to target and damage β pancreatic cells, reducing production of insulin and resulting in profound hyperglycemia.

Despite their hyperglycemia, mice did not present any significant fluctuation in their body weight at this early timepoint during the progression of diabetic injury as illustrated in Table 3 (25.9 ± 0.4g to 26.5 ± 0.5g for non-diabetic vehicle infused mice [*n*=5], 26.7 ± 0.6g to 27.6 ± 0.7g for non-diabetic SQ29548 infused mice [*n*=6], 25.5 ± 0.6g to 26.3 ± 0.6g for STZ vehicle infused mice [*n*=6], 26.0 ± 0.7g to 26.2 ± 0.9g for STZ SQ29548 infused mice [*n*=6]).

Similar observations applied to systolic blood pressure, and are illustrated in Table 3. A non-significant decrease was observed in systolic blood pressure from 122 ± 10mmHg to 111 ± 10mmHg in STZ vehicle infused mice (*n*=6) compared to 113 ± 7mmHg to 112 ± 5mmHg in control mice (*n*=5), and 120 ± 6mmHg to 112 ± 5mmHg in STZ SQ29548 infused mice (*n*=6) compared to 117 ± 7mmHg to 115 ± 5mmHg for control mice (*n*=6).

Results in our laboratory as well as in the literature reported significant variations in both of those parameters (body weight and systolic blood pressure) only in certain strains of mice with high levels of hyperglycemia for over 15 weeks. The absence of an effect on blood pressure and body weight results is in fact not surprising given the short duration of the study (Breyer, Bottinger *et al.* 2005; Gurley, Clare *et al.* 2006).

Table 3: STZ injected mice develop hyperglycemia without modulation of body weight nor systemic blood pressure.

Blood samples were collected at the time of sacrifice (4 weeks post-injections) by cardiac puncture. After centrifugation (13000rpm, 20min) of the samples, plasma was isolated and analysed with a glucometer. Staff members from the Animal Care and Veterinarian Services of the University of Ottawa measured body weight on a biweekly basis. This table references a comparison of weight pre-injections, after implantation of mini-pumps, and 4 weeks post-injections. Tail-cuff measurement of systolic blood pressure was carried out pre-injection/mini-pump implantation and at 4 weeks post-injections. Statistical analysis was done using two-way ANOVA in GraphPad Prism.

		$[Glucose]_{plasma}$ (mM)	**Body weight (g)**		**Systemic blood pressure (mmHg)**	
		4 weeks	Before injections	4 weeks	Before injections	4 weeks
- SQ29548	Na-Citrate	18.5 ± 0.9 (*n*=5)	25.9 ± 0.4 (*n*=5)	26.5 ± 0.5 (*n*=5)	113 ± 7 (*n*=5)	112 ± 5 (*n*=5)
	STZ	29.0 ± 2.1 *** (*n*=6)	25.5 ± 0.6 (*n*=6)	26.3 ± 0.6 (*n*=6)	122 ± 10 (*n*=6)	111 ± 10 (*n*=6)
+ SQ29548	Na-Citrate	18.0 ± 0.9 (*n*=6)	26.7 ± 0.6 (*n*=6)	27.6 ± 0.7 (*n*=6)	117 ± 7 (*n*=6)	115 ± 5 (*n*=6)
	STZ	26.7 ± 2.3 ** (*n*=6)	26.0 ± 0.7 (*n*=6)	26.2 ± 0.9 (*n*=6)	120 ± 6 (*n*=6)	112 ± 5 (*n*=6)

** $p < 0.01$ STZ+SQ29548 *vs* Na-Citrate+SQ29548; *** $p < 0.001$ STZ-SQ29548 *vs* Na-Citrate-SQ29548.

Type-1 diabetes and kidney damage.

Early on the type-1 diabetes pathophysiology is characterized by histological and hemodynamic changes including overall kidney hypertrophy, glomerular mesangial matrix accumulation, glomerular basement membrane thickening, and enhanced glomerular filtration rate (GFR) due to constriction of the efferent and dilatation of the afferent arterioles. In this section we will explore some of those variations and the impact of TP antagonist SQ29548 infusion in both non-diabetic and STZ-injected mice.

When the average of left and right kidney weights is normalized to the mouse body weight, it is possible to appreciate a phenomenon of kidney hypertrophy (Figure 8, A.). Kidneys from STZ-injected mice infused with vehicle showed significant hypertrophy ($p<0.01$, 9.8 ± 0.3mg/gBW [$n=6$]) when compared to their non-diabetic controls (6.7 ± 0.2mg/gBW [$n=5$]). In contrast, infusion with SQ29548 significantly prevented kidney hypertrophy in STZ-injected mice (8.2 ± 0.9mg/gBW [$n=6$]) compared to their non-diabetic controls (6.5 ± 0.3mg/gBW [$n=6$]).

Using representative pictures of periodic acid-Schiff (PAS) stained kidney sections obtained by light microscopy, it was possible to appreciate some glomerular hypertrophy in STZ-injected mice (Figure 8, B.2 and 4) compared to their respective controls (B.1 and 3) without other apparent glomerular damage. Analysis of glomerular surface area (Figure 8, C.) revealed a statistical difference ($p<0.01$) between STZ (3690 ± 139μm^2

[*n*=6]) and Na-Citrate (2964 ± 56μm^2 [*n*=5]) injected mice infused with vehicle. In contrast, STZ mice infused with SQ29548 did not show significant differences in glomerular surface area versus non-diabetic SQ29548 controls (STZ+SQ29548, 3621 ± 159μm^2 [*n*=6] versus Na-Citrate+SQ29548, 3244 ± 128μm^2 [*n*=6]).

Wilm's tumor 1 (WT-1) is a transcription factor expressed specifically in podocyte. Immunofluorescence staining of WT-1 on frozen sections of O.C.T. embedded kidneys can be used to quantify podocyte loss in models of glomerular injury. Figure 9 includes representative pictures without anti-WT-1 antibody (a,c,e,g) and with the primary antibody (b,d,f,h); as indicated in the figure, SQ29548 appears to prevent podocyte loss. Counts of WT-1 positive cells (Figure 9, B.) revealed a significant podocyte loss in STZ mice infused with the vehicle (p<0.01, average of 8.8 ± 0.3cells/glomerulus [*n*=3]; A.d) compared to their control (11.2 ± 0.8cells/glomerulus [*n*=3]; A.b). Mice infused with SQ29548 did not present any significant difference between Na-Citrate and STZ-injected mice (9.6 ± 0.3 cells/glomerulus [*n*=3]; A.f versus 10.0 ± 0.2cells/glomerulus [*n*=3]; A.h).

Podocin and nephrin are slit diaphragm proteins that can be downregulated in a variety of glomerular diseases including diabetic nephropathy. Furthermore, both TP receptor and COX-2 renal expression are often upregulated in diabetic nephropathy. Both podocin and nephrin mRNA expression levels were assessed by quantitative PCR along with expression of TP and COX-2 (Figure 10). Both COX-2 and TP cortical mRNA expression were not significantly changed in any of the four experimental groups (Na-

Citrate vehicle infused: 1.0 ± 0.1 arbitrary unit [*n*=3] for both; STZ vehicle infused: 1.2 ± 0.2a.u. [*n*=3] and 1.1 ± 0.1a.u. [*n*=3]; Na-Citrate SQ29548 infused: 1.1 ± 0.4a.u. [*n*=3] and 1.2 ± 0.1a.u. [*n*=3]; STZ SQ29548 infused 1.3 ± 0.8a.u. [*n*=3] and 1.0 ± 0.2a.u. [*n*=3] respectively). In contrast, nephrin and podocin mRNA expression were increased in the STZ SQ29548 infused mice with 2.3 ± 1.5a.u. (*n*=2) and 3.3 ± 1.4a.u. (*n*=3) versus 1.3 ± 0.6a.u. (*n*=2) and 1.2 ± 0.2a.u. (*n*=3) for their non-diabetic SQ29548 infused controls. The same effect did not occur in the vehicle infused mice with 1.2 ± 0.7a.u. (*n*=2) and 1.4 ± 0.2a.u. (*n*=3) for the STZ-injected mice versus 1.2 ± 0.6a.u. (*n*=2) and 1.0 ± 0.1a.u. (*n*=3) for the non-diabetic mice. Despite this apparent trend, no statistical significance was obtained.

Diabetes in mice results in profound osmotic diuresis. In order to examine the impact of TP antagonism upon urine output, mice were placed individually in metabolic cages for 24 hours. The individual urinary volume was collected and measured as illustrated in Figure 11. Induction of type-1 diabetes resulted in significant polyuria in the vehicle infused mice (16.9 ± 2.9ml/24hrs [*n*=6]) compared to non-diabetic mice (0.5 ± 0.1ml/24hrs [*n*=5]). However, although this polyuria was not completely normalized, it was significantly reduced by the TP antagonist administration in STZ-injected mice(8.3 ± 3.7ml/24hrs [*n*=6], $p<0.05$).

Glomerular filtration barrier damage is an early event in the STZ-induced model of type-1 diabetes. To examine the impact of TP antagonist administration on albuminuria, a

sample of urine was conserved for each specimen in order to assess albumin levels. In the case of this study, creatinine levels could not be determined due to levels below the sensitivity threshold of the test performed (data not shown). However, normalization to 24 hour volume (Figure 12) allowed detection of significant albuminuria in vehicle infused mice injected with STZ (466 ± 49µg/24hrs [n=6]) compared to the non-diabetic mice (177 ± 27µg/24hrs [n=5]), after 4 weeks of diabetes. Importantly, STZ-injected mice infused with SQ29548 exhibited a significant reduction in albuminuria (247 ± 67µg/24hrs [n=6], p<0.01 versus STZ vehicle infused mice).

A.

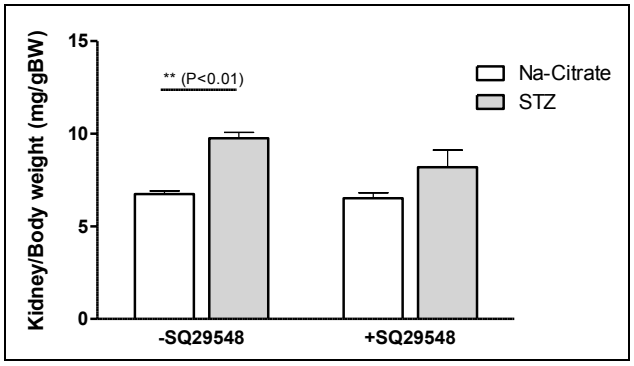

B.

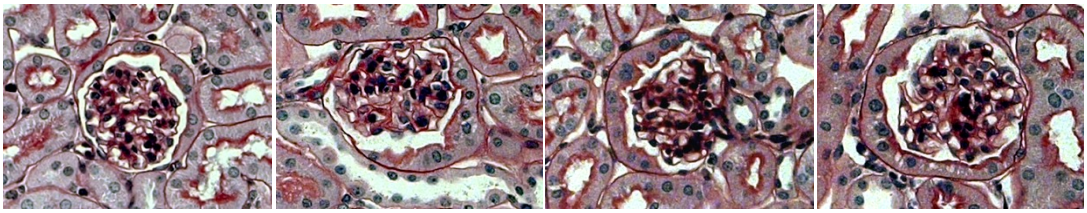

C.

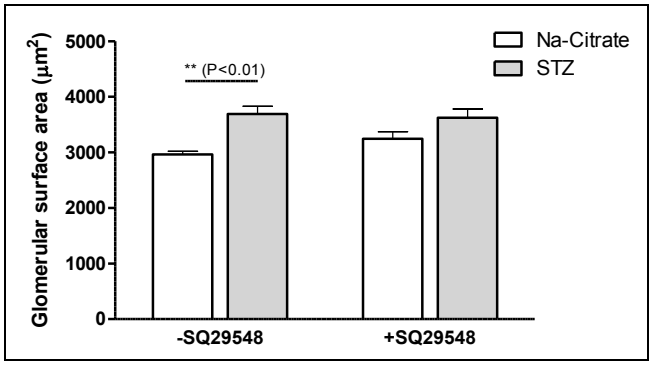

Figure 8: SQ29548 prevents kidney and glomerular hypertrophy.

Graph A illustrates the average of each kidney weight, measured at time of sacrifice, normalized to each mouse body weight, measured by the ACVS personal on the morning of the sacrifice. B. 4µm paraffin sections of kidney samples fixed for 24 hours in 4% paraformaldehyde, were stained by periodic acid-Schiff (PAS). Representative pictures were taken (B, 1: Na-Citrate-SQ29548, 2: STZ-SQ29548, 3: Na-Citrate+SQ29548, 4: STZ+SQ29548) and glomerular surface area of 20 glomeruli per mouse was measured using Zeiss Axiovision Rel 4.8 in a blinded manner (C). The statistical analysis was done using two-way ANOVA in GraphPad Prism.

A.

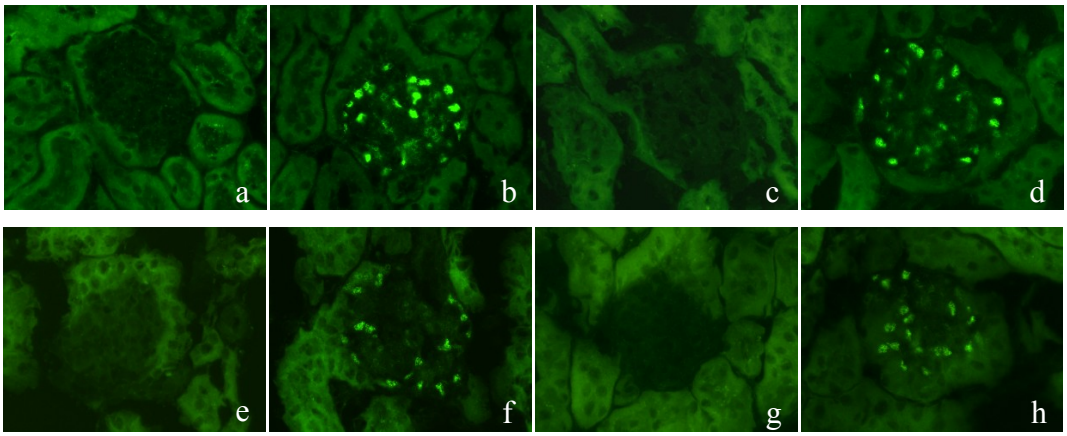

B.

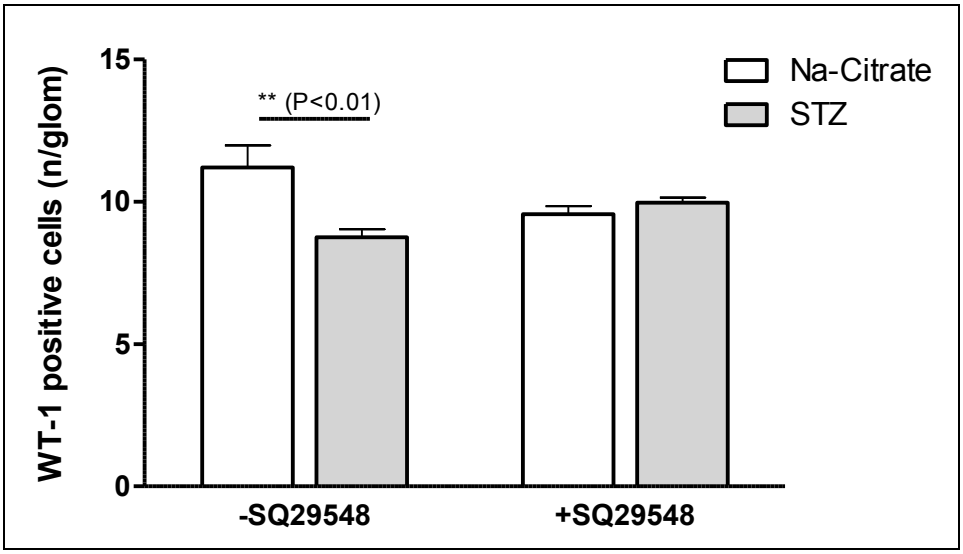

Figure 9: SQ29548 prevents podocyte loss.

8µm frozen sections of kidney samples embedded in O.C.T. were stained for detection of Wilm's tumor 1 (WT-1) and analyzed using Zeiss Axioskop 2 fluorescence microscope. A. Representative pictures illustrate all different conditions (b: Na-Citrate vehicle infused, d: STZ vehicle infused, f: Na-Citrate SQ29548 infused, h: STZ SQ29548 infused) and their controls (a,c,e,g: staining without primary antibody against WT-1). B. The analysis was done in a blinded manner using Zeiss Axiovision Rel 4.8 to determine the average of WT-1 positive cells per glomeruli, over 20 glomeruli per mouse. The statistical analysis was done using two-way ANOVA in GraphPad Prism.

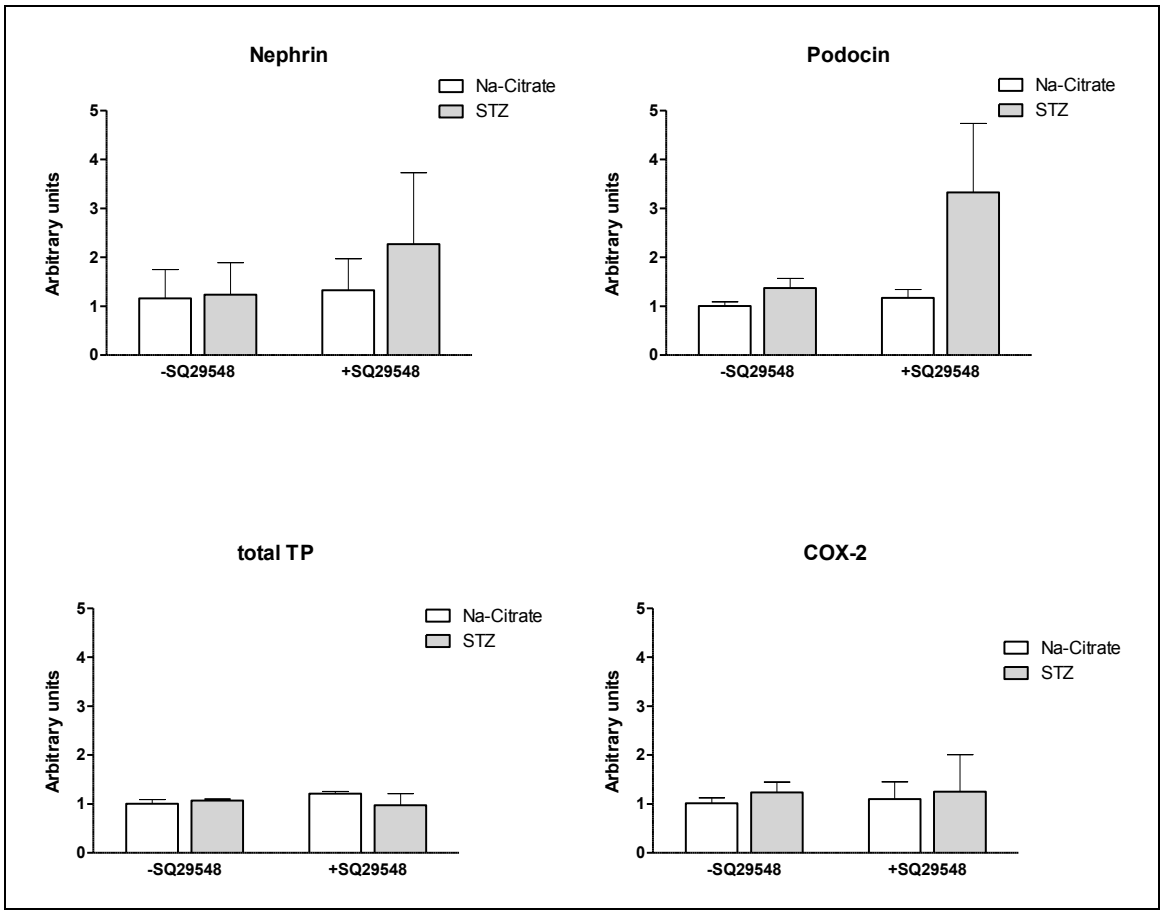

Figure 10: Cortical mRNA expression of cytoskeletal remodeling markers.

RNA was extracted from approximately 20mg of snap frozen cortex as described in materials and methods, and 1µg was reverse transcribed before analysis by quantitative PCR. Primers for nephrin, podocin, total TP, and COX-2 were used as well as β-actin as a reaction control. Each primer set was normalized to its reaction control β-actin before being normalized again to the average of Na-Citrate vehicle infused mice. Arbitrary units are determined by calculation of $2^{-\Delta\Delta Ct}$. Statistical analysis was done using two-way ANOVA in GraphPad Prism.

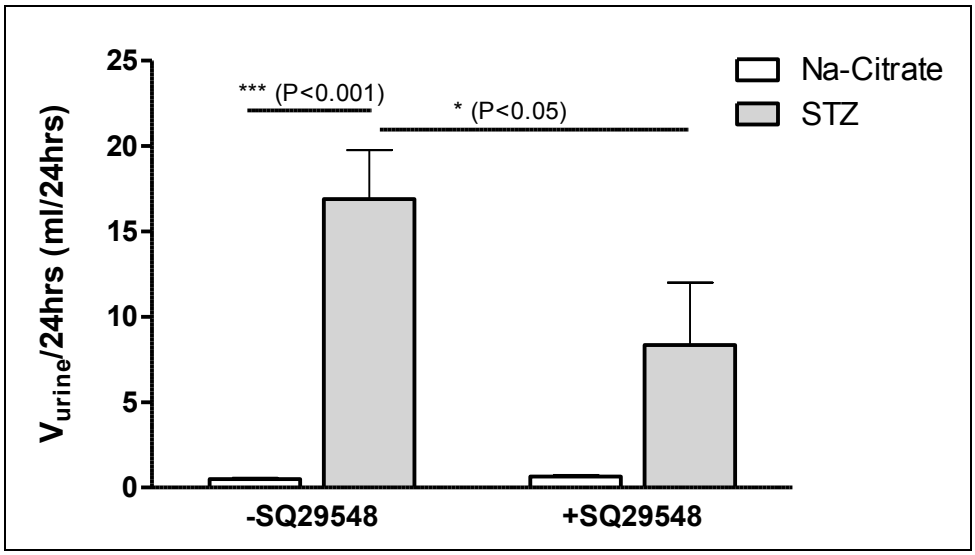

Figure 11: SQ29548 reduces STZ induced polyuria.

At 4 weeks post-injections, mice were placed into metabolic cages for 24 hours. Urine was collected and the volume obtained was measured. The statistical analysis of the data was done using two-way ANOVA in GraphPad Prism.

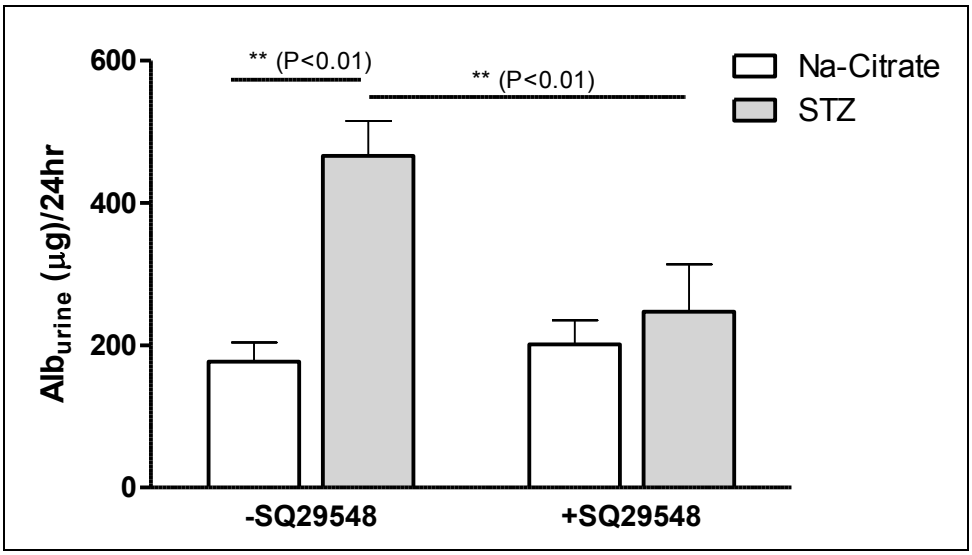

Figure 12: SQ29548 prevents the appearance of albuminuria after 4 weeks of diabetes.

24 hour urine collections were assayed for albumin content. Dilutions of 1:1000 for Na-Citrate injected mice and 1:2000 for STZ-injected mice allowed a proper estimation. Values were normalized to 24 hour volume collected (Figure 11). The statistical analysis of the data was done using two-way ANOVA in GraphPad Prism.

Chapter III: Results

Part 2: Diabetic nephropathy and podocyte-specific thromboxane receptor overexpression.

2.1 Characterization of TP^{pod+} model.

Our results presented in the previous chapter clearly demonstrated a protective effect of TP receptor antagonist administration upon glomerular damage and albuminuria in the STZ-induced type-1 diabetic nephropathy mouse model. These findings strongly suggest that thromboxane A_2/TP receptor signalling contributes to filtration barrier injury in diabetes. However, these findings do not address the question of the precise location of the deleterious thromboxane A_2/TP receptor actions. A number of observations allowed us to hypothesize that the podocyte is the target of such thromboxane A_2/TP receptor activity: 1) podocytes express TP receptors (Bek, Nusing *et al.* 1999); 2) exposure of cultured podocytes to diabetic conditions (i.e., high glucose and mechanical stretch) induces both COX-2 and TP receptor expression; and 3) podocyte injury occurs early in diabetic nephropathy and is associated with albuminuria.

In order to test our hypothesis, mice overexpressing the mouse TP receptor specifically in podocytes (TP^{pod+}) were generated by Roya Shaji, a previous Masters student in the laboratory, with the help of the Kidney Research Centre staff. Details of construct and transgenic mouse development can be found in Ms. Shaji's thesis (Shaji 2011). Briefly, a mouse TP receptor cDNA construct containing N- and C-terminal hemagglutinin (HA) epitope tags was obtained from Dr. Robert Spurney (Duke University). This cDNA was cloned immediately downstream of a 8.3 kb fragment of the mouse *NPHS1* promoter to allow for podocyte-specific expression. The transgene was excised by restriction enzyme

digestion, purified, and injected into FVB/n oocytes to generate transgenic founders. PCR-based genotyping of tail snip DNA identified six founders. Quantitative RT-PCR using HA-tag and TP-specific primers was performed on renal total RNA obtained from offspring of the founders to determine those lines with the highest transgene expression. Immunofluorescence using a HA antibody confirmed podocyte-specific expression.

We next set out to determine whether the transgenic TP receptor was functional. A first approach consisted of isolating glomeruli, letting podocytes expand on coverslips to provide some attachment, and analyzing intracellular calcium influx in response to TP agonist U46619 stimulation using live-imaging. The response obtained with calcium ionophore A23187 was used as a positive control. As shown in Figure 13, glomeruli obtained from TP^{pod+} mice did show indications of intracellular Ca^{2+} elevations in response to the TP agonist U46619, whereas those from non-transgenic mice were generally unresponsive (Figure 14). The calcium ionophore A23187 elicited Ca^{2+} elevations in glomeruli from both TP^{pod+} and non-transgenic mice. Although this method appeared promising, the degree of reproducibility of the results was low. Very few of either the transgenic or non-transgenic glomerular preparations yielded positive results for either U46619 or A23187 suggesting that the experimental conditions were not optimal.

As an alternative approach we determined the mRNA expression of downstream effectors of TP/TXA_2 pathway when TP is stimulated with TP agonist U46619. Effectors have

been selected according to the results of a microarray chip assay of conditionally immortalized mouse podocyte stimulated for 2 and 24 hours with 1µM of U46619 (Laura MacLoed, unpublished results). After 2 hours of stimulation, NCK associated protein 5-like (Nckap5l) mRNA expression was 3-fold downregulated, whereas superoxide dismutase 1 (Sod1) mRNA expression was more than 3 fold upregulated (data not shown).

RNA extracted from glomeruli stimulated for 2 hours with U46619 did not reveal any significant change according to quantitative PCR results (Figure 15). Despite a tendency of Nckap5l to be 3 times upregulated in stimulated transgenic mice with 12.8 ± 12.3arbitrary units (a.u., n=5) versus 4.3 ± 3.7a.u. (n=5) for the non-stimulated transgenic mice, no difference has been observed in the non-transgenic mice (3.5 ± 2.2a.u. after stimulation [n=5] versus 3.2 ± 2.4a.u. for controls [n=5]). Due to Nckap5l possible interaction in actin cytoskeleton remodelling, we looked at the mRNA expression of nephrin. In both non-transgenic and TP^{pod+} mice, nephrin expression showed a tendency to be downregulated when stimulated with TP agonist (0.8 ± 0.1a.u. [n=4] and 0.6 ± 0.1a.u. [n=4] respectively) compared to their respective controls (1.7 ± 1.1a.u. [n=4] and 1.1 ± 0.3a.u. [n=4]).

Superoxide dismutase-1 is the other downstream effector of TP/TXA_2 pathway studied. Here again, no statistical difference was detected between non-transgenic stimulated (1.7

± 0.3a.u. [*n*=5]) and non stimulated controls (1.2 ± 0.3a.u. [*n*=5]) nor between TP^{pod+} stimulated (1.5 ± 0.4a.u. [*n*=5]) and their non stimulated controls (1.1 ± 0.3a.u. [*n*=5]).

Levels of cyclooxygenase 2 (COX-2) and total TP were also assessed and both showed the same trend: there was a tendency to increase with stimulation in non-transgenic mice (1.6 ± 0.3a.u. [*n*=3] and 1.5 ± 0.7a.u. [*n*=4] respectively) compared to their non stimulated controls (1.0 ± 0.2a.u. [*n*=3] and 1.3 ± 0.5a.u. [*n*=4] respectively) and a slight decrease with stimulation in TP^{pod+} mice (1.0 ± 0.1a.u. [*n*=3] and 0.9 ± 0.3a.u. [*n*=4] respectively) compared to their non stimulated controls (1.2 ± 0.4a.u. [*n*=3] and 1.1 ± 0.3a.u. [*n*=4] respectively).

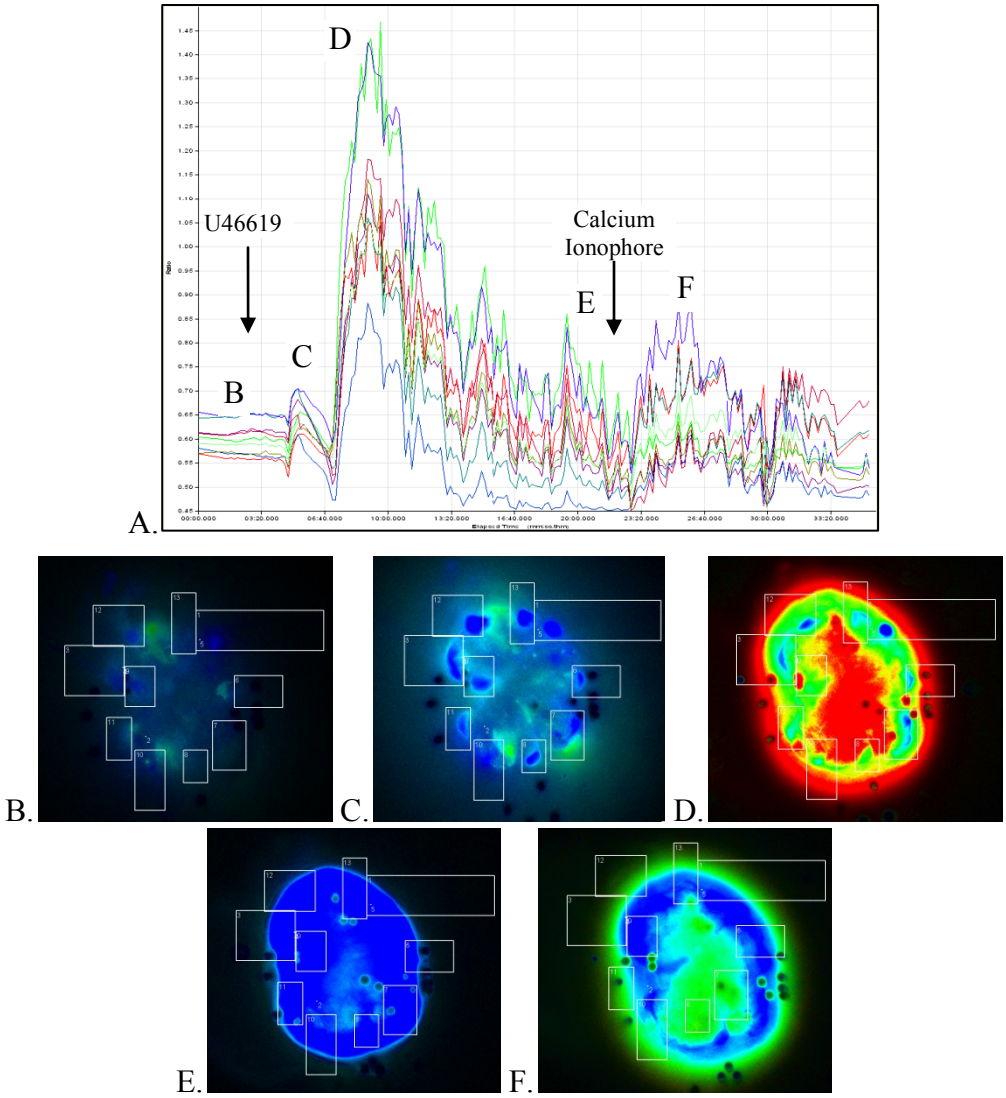

Figure 13: TP agonist induces intracellular Ca^{2+} release in TP^{pod+} mice glomerulus.

48 hour isolated glomeruli were seeded on collagen I coated coverslips and loaded with Fura-2AM for 45 minutes before being allowed to equilibrate (B). Glomeruli were then stimulated with the TP agonist U46619 (1µM) resulting in an induction of intracellular calcium elevation (C-D) 6 minutes after exposure to U46619. Original global calcium level could not be reached again (E) and stimulation with positive control calcium ionophore A23187 (2µM) induced a lower level of response (F). The ratio of free (340nm) versus Fura-2AM bound (380nm) calcium was followed and quantified using live imaging (A).

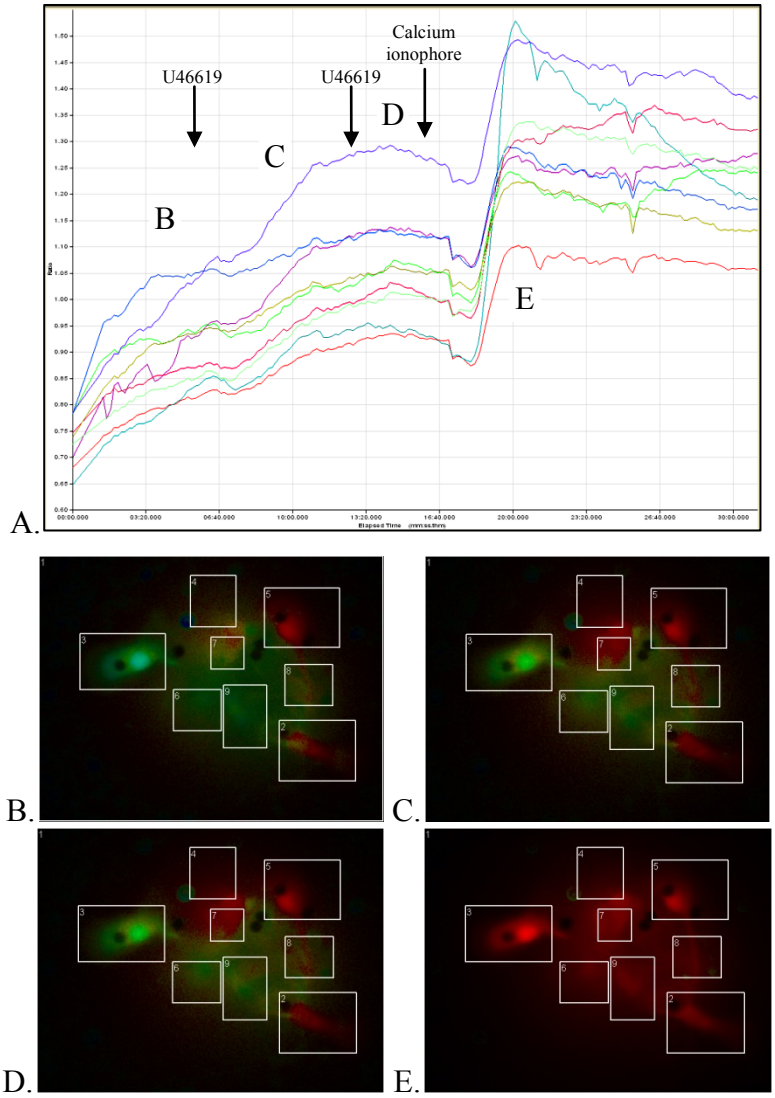

Figure 14: TP agonist stimulation induces low intracellular Ca^{2+} release in non-transgenic mice glomerulus.

Isolated glomeruli were seeded on collagen I coated coverslips for 48 hours, loaded with Fura-2AM for 45 minutes before being allowed to equilibrate (B). Stimulation with 1µM of TP agonist U46619 failed to induce intracellular calcium elevation (C-D). 2µM of positive control calcium ionophore A23187 induced a global response (E). The ratio of free (340nm) versus Fura-2AM bound (380nm) calcium was followed and quantified using live imaging (A).

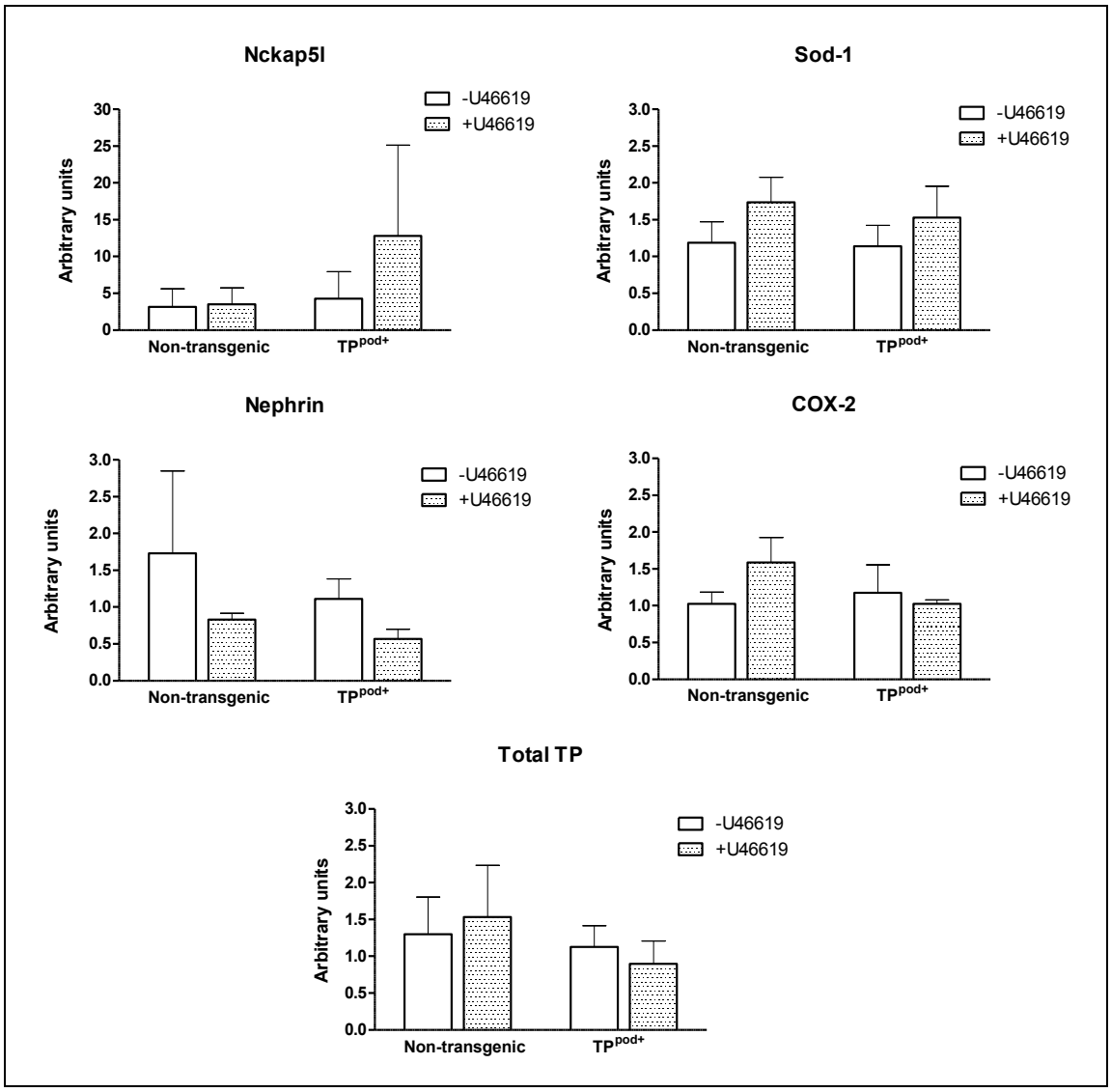

Figure 15: mRNA expression of TP downstream effectors and other targeted genes.

1µg of RNA, extracted out of glomeruli stimulated or not with U46619, was submitted to DNase I treatment and reverse transcription before quantitative PCR was performed to assess levels of TP/TXA_2 downstream effectors: Nckap5l and Sod-1, as well as Nephrin, COX-2, and total TP. Each Ct value was normalized to $Ct_{\beta\text{-actin}}$ value to obtain ΔCt. ΔΔCt was calculated as normalization of each ΔCt to the average of ΔCt for non-transgenic or TP^{pod+} mice, for this gene. The arbitrary units resulted in the calculation: $2^{-(\Delta\Delta Ct)}$. Further statistical analysis was done using two-way ANOVA in GraphPad Prism.

2.2 Low dose of Streptozotocin: 50mg/kg/day.

We next tested the impact of podocyte-specific TP receptor overexpression in the STZ-induced mouse model of diabetic nephropathy. For this purpose, 10 week old FVB/n males (i.e., non-transgenic and TP^{pod+} mice) were injected with either 50mg/kg/day STZ or with vehicle (Na-Citrate).

Confirmation of type-1 diabetes

As previously described in the antagonist study, injections of STZ-induced an increase in plasma glucose concentration without any significant differences between non-transgenic and TP^{pod+} mice: 30.0 ± 2.1mM (*n*=5) and 28.8 ± 3.2mM (*n*=4) respectively, when compared to their respective non-diabetic controls: 14.9 ± 1.1mM (*n*=4) and 8.1 ± 0.1mM (*n*=2) (Table 4).

As depicted in Table 4, the trend of body weight over the 11 weeks of type-1 induced diabetes demonstrated that mice tended to gain weight but no statistical difference was observed between STZ non-transgenic mice (24.1 ± 0.7g to 26.2 ± 0.6g to 27.0 ± 0.6g [*n*=5]) versus their non-diabetic controls (24.7 ± 1.3g to 28.0 ± 1.3g to 29.9 ± 1.6g [*n*=4]) nor between STZ TP^{pod+} mice (24.1 ± 0.6g to 25.0 ± 1.7g to 27.6 ± 1.3g [*n*=4]) versus

their non-diabetic controls (24.5 ± 0.6g to 27.5 ± 0.6g to 28.0 ± 0.3g [*n*=2]) or between non-transgenic and TP^{pod+} mice.

STZ-induced diabetes had no appreciable impact upon systolic blood pressure in either non-transgenic or TP^{pod+} mice (Table 4). Despite the tendency of blood pressure to increase with age, no statistical difference was found between any of the groups.

Table 4: Low dose STZ induce hyperglycemia without significant modulation of body weight nor systemic blood pressure.

Blood samples were collected at the time of sacrifice, 11 weeks post-injections, by cardiac puncture. Plasma was isolated after centrifugation (13000rpm, 20min) of the samples. Glycemia was determined using the OneTouch Ultra2 glucometer (Lifescan Inc., Milpitas, CA). Staff of the ACVS of the University of Ottawa measured body weight on a biweekly basis. This table illustrates a comparison of weight pre-injections, after eight weeks of diabetes, prior to metabolic cages isolation, and the morning of sacrifice, 11 weeks post-injections. Tail-cuff measurement of systolic blood pressure were done pre-injection and at 8 weeks post-injections. Statistical analysis was done using one-way and two-way ANOVA in GraphPad Prism.

		$[Glucose]_{plasma}$ (mM)	**Body weight (g)**			**Systemic blood pressure (mmHg)**	
		11 weeks	Before injections	8 weeks	11 weeks	Before injections	8 weeks
Non-transgenic	Na-Citrate	14.9 ± 1.1 (*n*=4)	24.7 ± 1.3 (*n*=4)	28.0 ± 1.3 (*n*=4)	29.9 ± 1.6 (*n*=4)	110 ± 2 (*n*=4)	115 ± 13 (*n*=4)
	STZ	30.0 ± 2.1 *** (*n*=5)	24.1 ±0.7 (*n*=5)	26.2 ±0.6 (*n*=5)	27.0 ±0.6 (*n*=5)	106 ± 2 (*n*=5)	112 ± 6 (*n*=5)
TP^{pod+}	Na-Citrate	8.1 ± 0.1 (*n*=2)	24.5 ± 0.6 (*n*=2)	27.5 ± 0.6 (*n*=2)	28.0 ± 0.3 (*n*=2)	97 ± 4 (*n*=2)	110 ± 10 (*n*=2)
	STZ	28.8 ± 3.2 *** (*n*=4)	24.1 ± 0.6 (*n*=4)	25.0 ± 1.7 (*n*=4)	27.6 ± 1.3 (*n*=4)	111 ± 6 (*n*=4)	122 ± 6 (*n*=4)

*** $p < 0.001$ STZ injected mice *vs* Na-Citrate injected mice.

Indications of diabetic renal injury in STZ TP^{pod+} mice.

As shown in Figure 16A, kidney hypertrophy was slightly, but significantly, reduced in STZ TP^{pod+} mice as compared to non-transgenic STZ mice (9.7 ± 1.4mg/gBW [*n*=4] versus 11.0 ± 1.0mg/gBW [*n*=5] respectively).

In contrast, glomerular surface area (Figure 16, C.) was similarly increased for both non-transgenic and TP^{pod+} mice injected with STZ (4760 ± 120.5μm^2 [*n*=5] and 5073 ± 283.3μm^2 [*n*=4], when compared to their respective non-diabetic controls: 3812 ± 126.4μm^2 [*n*=4] and 3817 ± 67.55μm^2 [*n*=2] respectively). Representative images (Figure 16,B.) illustrate glomerular histology in each group of non-transgenic (images 1 and 2) and TP^{pod+} mice (images 3 and 4). At this relatively early timepoint in the progression of diabetes, no major histological damage was observed in either group.

Podocyte numbers were not reduced in any of the STZ groups (9.1 ± 0.6cells/glomerulus [*n*=5] for non-transgenic mice; 9.9 ± 1.0cells/glomerulus [*n*=4] for TP^{pod+} mice) compared to non-diabetic mice (10.5 ± 0.9cells/glomerulus [*n*=4] for non-transgenic mice; 11.1 ± 0.1cells/glomerulus [*n*=2] for TP^{pod+} mice) as determined by the number of WT-1 positive podocytes identified on glomerular cross sections (Figure 17).

Urinary volume collected after the 24 hour period indicated that when compared to their non-diabetic controls (0.5 ± 0.1ml/24hrs [*n*=4] for non-transgenic, and 0.5 ± 0.1ml/24hrs

[*n*=2] for TP^{pod+}) both diabetic groups demonstrated similar polyuria (21.5 ± 5.1ml/24hrs [*n*=5] for non-transgenic versus 21.1 ± 7.6ml/24hrs [*n*=4] for TP^{pod+} mice).

In order to assess if the integrity of the glomerular filtration barrier was impaired, the levels of albuminuria were measured and normalized to urine volume per 24 hour. Similar statistically significant increases in albuminuria were observed for both STZ non-transgenic and STZ TP^{pod+} mice (1264 ± 653.6µg/24hrs [*n*=5] and 674.0 ± 265.5µg/24hrs [*n*=4] respectively).

It has to be noted that in a two-way ANOVA statistical analysis, the number of mice represents a variable. The fact that only 2 mice constituted the TP^{pod+} non-diabetic group could explain the absence of statistical significance in the analysis of kidney hypertrophy (Figure 16) and 24 hour urine volume (Figure 18). Another set of mice was injected with the same dose of STZ in order to complete the study. Distinct results indicated that even if those mice developed a more moderate hyperglycemia they presented no sign of diabetic nephropathy (no sign of kidney or glomerular hypertrophy, really mild polyuria and reasonable levels of albuminuria) (refer to supplementary data in appendices Figure 28 to Figure 34).

A.

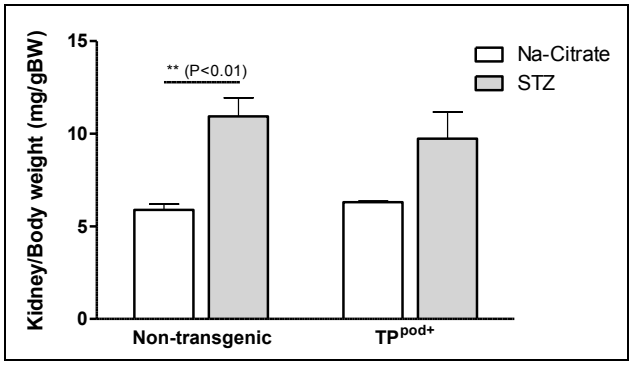

B.

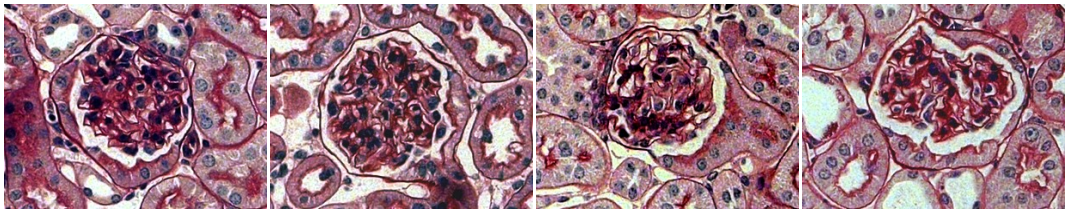

C.

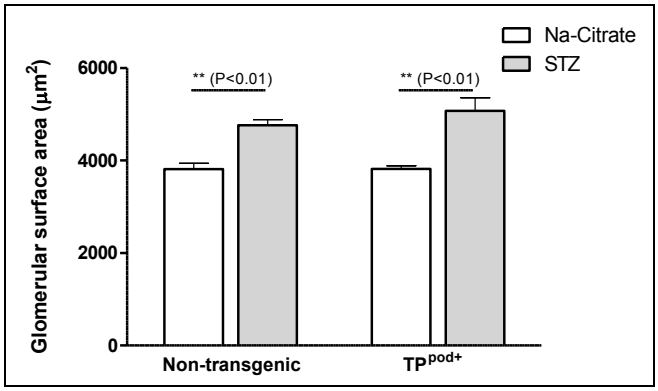

Figure 16: Low dose of STZ induces minor renal and glomerular pathology.

The average of each kidney weights has been normalized to each mouse body weight measured by ACVS personal on the morning of sacrifice (A). 4µm paraffin sections of kidney samples fixed for 24 hours in 4% paraformaldehyde were stained by periodic acid-Schiff (PAS). Representative pictures (B, 1: non-transgenic Na-Citrate, 2: non-transgenic STZ, 3: TP^{pod+} Na-Citrate, 4: TP^{pod+} STZ) were taken and glomerular diameter of 20 glomeruli per mouse was measured using Zeiss Axiovision Rel 4.8 in a blinded manner (C). The statistical analysis was done using two-way ANOVA in GraphPad Prism.

A.

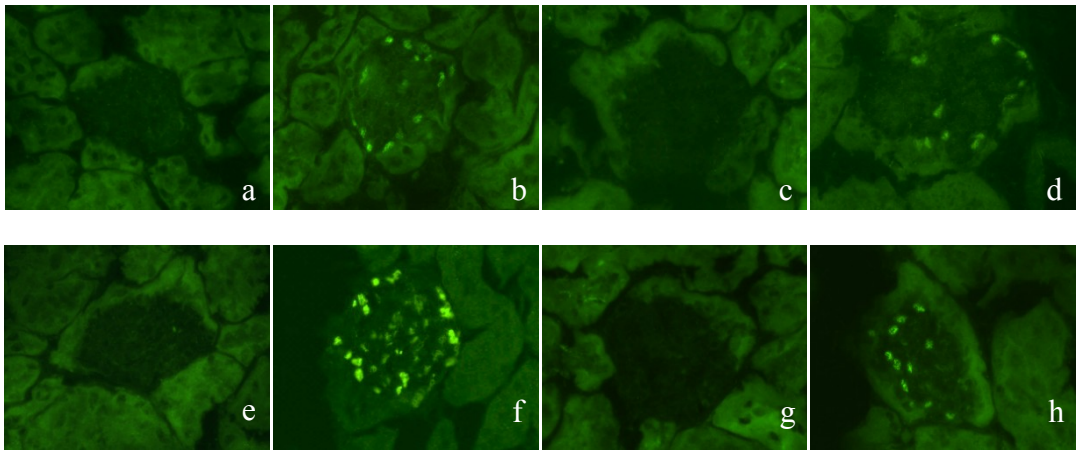

B.

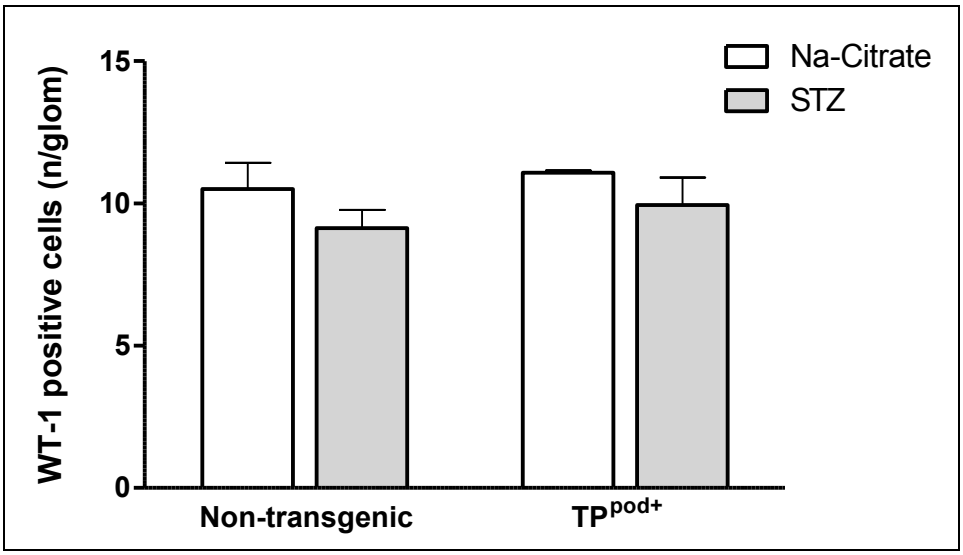

Figure 17: Low dose of STZ tend to induce podocyte loss.

8µm frozen sections of kidney samples embedded in O.C.T. were stained for detection of Wilm's tumor 1 (WT-1) and analyzed using Zeiss Axioskop 2 fluorescence microscope. A. Representative pictures illustrate all different conditions (b: non-transgenic Na-Citrate injected, d: non-transgenic STZ-injected, f: TP^{pod+} Na-Citrate injected, h: TP^{pod+} STZ-injected) and their controls (a,c,e,g: staining without primary antibody against WT-1). B. The analysis was done in a blinded manner using Zeiss Axiovision Rel 4.8 to determine the average of WT-1 positive cells per glomeruli, over 20 glomeruli per mouse. The statistical analysis was done using two-way ANOVA in GraphPad Prism.

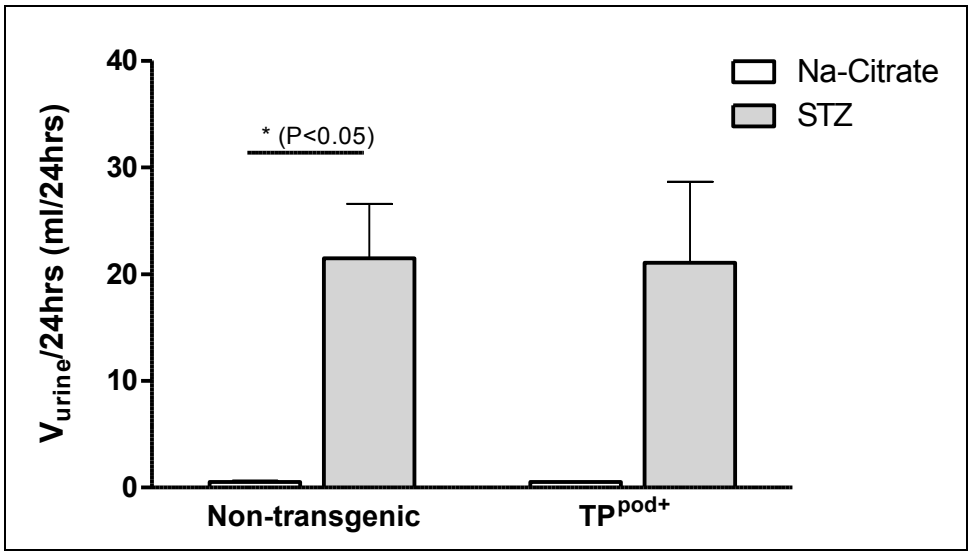

Figure 18: Type-1 diabetes induces polyuria in low dose STZ injected mice.

At eight weeks post-injections, mice were placed into metabolic cages for 24 hours. Urine was collected and the volume obtained was measured. Statistical analysis of the data was done using two-way ANOVA in GraphPad Prism.

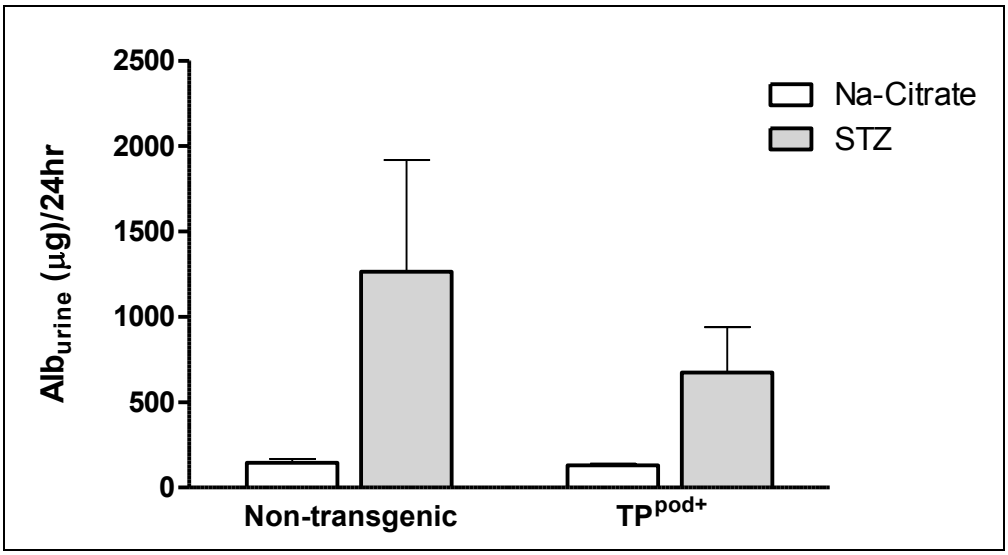

Figure 19: Glomerular filtration barrier damages in low dose STZ injected mice.

24 hour urine collection samples were submitted to albumin quantification using the Mouse Albumin ELISA Kit (Bethyl Laboratories Inc.) and have been normalized to 24 hour volume. Statistical analysis of the data was done using two-way ANOVA in GraphPad Prism.

2.3 Medium dose of Streptozotocin: 75mg/kg/day.

Since results of the experiment with a low dose of STZ resulted in a very minor level of diabetic renal injury, it was decided to repeat the experiments with the same model of diabetic nephropathy but with a higher dose of STZ: 75mg/kg/day.

Confirmation of type-1 diabetes

As previously described in the antagonist study, both non-transgenic and TP^{pod+} diabetic mice demonstrated a significant increase in their blood glucose (45.2 ± 1.2mM [*n*=11] and 43.5 ± 0.8mM [*n*=17] respectively) compared to their respective non-diabetic controls (14.2 ± 0.8mM [*n*=5] and 16.3 ± 0.6mM [*n*=9] respectively), but no significant difference was observed between TP^{pod+} and non-transgenic mice (Table 5).

Whereas non-diabetic mice tended to gain weight throughout the experiment: 26.7 ± 1.0g, 28.7 ± 0.8g and 29.7 ± 1.0g for non-transgenic mice (baseline, 8weeks and 11 weeks [*n*=10]) and 24.5 ± 0.6g, 27.4 ± 0.7g and 28.8 ± 0.8g for TP^{pod+} mice (*n*=14), mice injected with STZ lost weight by eight weeks of diabetes: 26.9 ± 0.4g, 24.7 ± 0.4g and 26.0 ± 0.5g for non-transgenic mice (*n*=18) and 25.5 ± 0.5g, 23.7 ± 0.4g and 25.2 ± 0.6g for TP^{pod+} mice (*n*=23). However none of those changes were statistically significant when STZ-injected mice were compared with their non-diabetic control mice (Table 5).

Systolic blood pressure tended to increase slightly in both groups of STZ-injected mice (Table 5): 121 ± 3mmHg to 127 ± 3mmHg in the non-transgenic mice (n=16), and 119 ± 3mmHg to 122 ± 4mmHg in the TP^{pod+} mice (n=22), over 8 weeks of diabetes. In contrast, non-diabetic mice exhibited a slight decrease in systolic blood pressure from 120 ± 5mmHg to 117 ± 4mmHg in the non-transgenic mice (n=10) and from 116 ± 4mmHg to 112 ± 3mmHg in the TP^{pod+} mice (n=14). However, none of these changes were statistically significant.

Table 5: Medium dose STZ induces hyperglycemia without significant modulation of body weight nor systemic blood pressure.

Blood samples were collected at the time of sacrifice, 11 weeks post-injections, by cardiac puncture. Plasma was isolated after centrifugation (13000rpm, 20min) of the samples. 70µl of each sample was sent for glucose quantification (IDEXX Laboratories, Markham, ON). ACVS personal of the University of Ottawa measured body weight on a biweekly basis. This table illustrates a comparison of weight pre-injections, after eight weeks of diabetes, prior to metabolic cages isolation, and the morning of sacrifice at 11 weeks post-injections. Tail-cuff measurement of systolic blood pressure were done pre-injection and at 8 weeks post-injections. Statistical analysis was done using one-way and two-way ANOVA in GraphPad Prism.

		$[Glucose]_{plasma}$ (mM)	**Body weight (g)**			**Systemic blood pressure (mmHg)**	
		11 weeks	Before injections	8 weeks	11 weeks	Before injections	8 weeks
Non-transgenic	Na-Citrate	14.2 ± 0.8 (*n*=5)	26.7 ± 1.0 (*n*=10)	28.7 ± 0.8 (*n*=10)	29.7 ± 1.0 (*n*=10)	120 ± 5 (*n*=10)	117 ± 4 (*n*=10)
	STZ	45.2 ± 1.2 *** (*n*=11)	26.9 ± 0.4 (*n*=18)	24.7 ± 0.4 (*n*=18)	26.0 ± 0.5 (*n*=18)	121 ± 3 (*n*=16)	127 ± 3 (*n*=16)
TP^{pod+}	Na-Citrate	16.3 ± 0.6 (*n*=9)	24.5 ± 0.6 (*n*=14)	27.4 ± 0.7 (*n*=14)	28.8 ± 0.8 (*n*=14)	116 ± 4 (*n*=14)	112 ± 3 (*n*=14)
	STZ	43.5 ± 0.8 *** (*n*=17)	25.5 ± 0.5 (*n*=23)	23.7 ± 0.4 (*n*=23)	25.2 ± 0.6 (*n*=23)	119 ± 3 (*n*=22)	122 ± 4 (*n*=22)

*** $p < 0.001$ STZ injected mice *vs* Na-Citrate injected mice.

Indications of diabetic renal injury in STZ TP^{pod+} mice.

Kidney from both non-transgenic and TP^{pod+} STZ-injected mice were significantly hypertrophic (10.9 ± 0.4mg/gBW [*n*=18] for and 10.6 ± 0.4mg/gBW [*n*=23] respectively, Figure 20, A.) when compared to their respective healthy controls (6.2 ± 0.2mg/gBW [*n*=10] and 6.0 ± 0.1mg/gBW [*n*=14]).

As expected, analysis of PAS stained kidney sections (Figure 20, C.) revealed statistically significant glomerular hypertrophy between both non-transgenic and TP^{pod+} diabetic mice (5658 ± 454μm^2 [*n*=5] and 5618 ± 286μm^2 [*n*=5]) and their respective non-diabetic controls (3730 ± 187μm^2 [*n*=5] and 3713 ± 190μm^2 [*n*=5]), but no statistical difference was observed between diabetic TP^{pod+} and non-transgenic mice. Representative histological images of PAS stained kidney sections illustrated glomerular hypertrophy with some sclerosis in STZ-injected mice (Figure 20, B.2 and 4) compared to their respective non-diabetic controls (1 and 3). No apparent differences were noted between non-transgenic and TP^{pod+} diabetic mice.

Sclerosis in glomeruli rendered the analysis of the WT-1 staining more challenging and tended to obscure the fluorescent immunostaining signal (Figure 21). However, results indicated no statistical difference between non-transgenic diabetic and non-diabetic mice (7.4 ± 0.3cells/glomerulus [*n*=5] and 7.2 ± 0.3cells/glomerulus [*n*=5] respectively), nor

between TP^{pod+} diabetic and non-diabetic mice, despite a slight podocyte loss tendency (7.5 ± 0.6cells/glomerulus [*n*=5] and 8.4 ± 1.0cells/glomerulus [*n*=5]).

As mentioned in the antagonist study, quantitative RT-PCR determination of podocin mRNA expression is recognized as a marker of podocyte cytoskeletal remodeling (Figure 22). No difference was observed at the baseline levels when comparing non-transgenic and TP^{pod+} mice injected with vehicle: 1.1 ± 0.3a.u. (*n*=3) and 0.8 ± 0.2a.u. (*n*=3). A similar increase in podocin expression to 2.1 ± 0.7a.u. (*n*=3) and 2.2 ± 0.5a.u. (*n*=3) respectively was quantified but was not statistically significant. We next determined whether the diabetic state was able to induce renal TP receptor expression. Cortical TP mRNA levels were induced to similar levels in non-transgenic diabetic mice (3.2 ± 0.6a.u. [*n*=3] versus 1.6 ± 1.1a.u. [*n*=3] for the non-diabetic control mice) and TP^{pod+} diabetic mice (2.8 ± 0.8a.u. [*n*=3] versus 1.4 ± 0.7a.u. [*n*=3] for the non-diabetic control mice). Cortical COX-2 mRNA expression tended to increase in non-transgenic diabetic mice (2.4 ± 1.8a.u. [*n*=3] versus 1.7 ± 0.9a.u. [*n*=3] for the non-diabetic controls). However, TP^{pod+} diabetic mice did not demonstrate a similar tendency (2.0 ± 1.2a.u. [*n*=3] versus 1.9 ± 1.2a.u. [*n*=3] for the non-diabetic controls).

In order to verify that diabetes was inducing equivalent polyuria in the mice, 24 hour urinary volumes were measured (Figure 23) at 8 weeks post-injection. Polyuria was observed in STZ-injected mice (31.7 ± 2.0ml for non-transgenic [*n*=16] versus 26.0 ± 2.5ml for TP^{pod+} mice [*n*=22]) compared with their non-diabetic controls (0.5 ± 0.1ml

[*n*=10] and 0.5 ± 0.1ml [*n*=14] respectively). Once again, no statistical difference was observed between non-transgenic and TP^{pod+} mice.

As glomerular hyperfiltration is a characteristic of early diabetic nephropathy, we assessed glomerular filtration rate levels in response to STZ-induced diabetes. Induction of type-1 diabetes resulted in higher GFR for both non-transgenic and TP^{pod+} mice (16.0 ± 2.5µl/min/gBW [*n*=5] and 14.1 ± 2.0µl/min/gBW [*n*=5] respectively) compared to their non diabetic controls (6.5 ± 1.4µl/min/gBW [*n*=5] and 6.8 ± 1.3µl/min/gBW [*n*=5] respectively) at eleven weeks post-injection (Figure 24). A slight statistical difference between TP^{pod+} and non-transgenic mice was observed since the *p* value is inferior to 0.01 between non-diabetic and diabetic non-transgenic mice, and inferior to 0.05 between non-diabetic and diabetic TP^{pod+} mice.

In order to assess the impact of podocyte-specific TP receptor overexpression on overall glomerular filtration barrier damage in STZ-induced diabetes, we collected 24 hour urine samples and assayed for albumin. When normalized to urinary creatinine levels, albuminuria was significantly higher in STZ-injected TP^{pod+} mice (1586 ± 324µg/mg [*n*=20] compared to non-diabetic mice 113 ± 24µg/mg [*n*=14], $p<0.001$) than in STZ-injected non-transgenic mice (1229 ± 149µg/mg [*n*=15] compared to the non-diabetic mice 263 ± 59µg/mg [*n*=9], $p<0.05$). The same characteristic was not found when normalized to 24 hour urine volume, but both STZ-injected non-transgenic and TP^{pod+} mice developed a significant albuminuria (1634 ± 285µg/24hrs [*n*=16] and 1465 ±

227μg/24hrs [*n*=22] respectively) when compared to their non-diabetic controls (105 ± 20μg/24hrs [*n*=10] and 105 ± 15μg/24hrs [*n*=14] respectively). Therefore, STZ-induced diabetes resulted in similar levels of albuminuria in both non-transgenic and TP^{pod+} mice (Figure 25).

A.

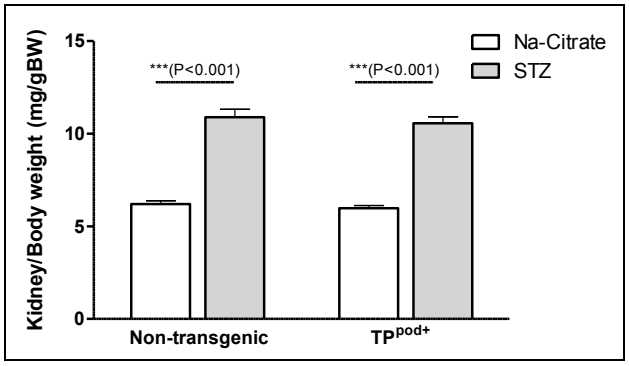

B.

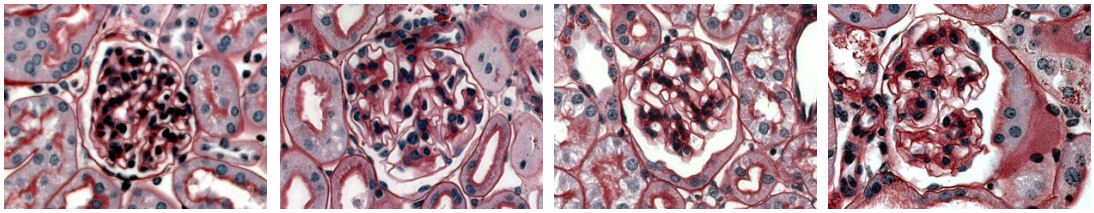

1 2 3 4

C.

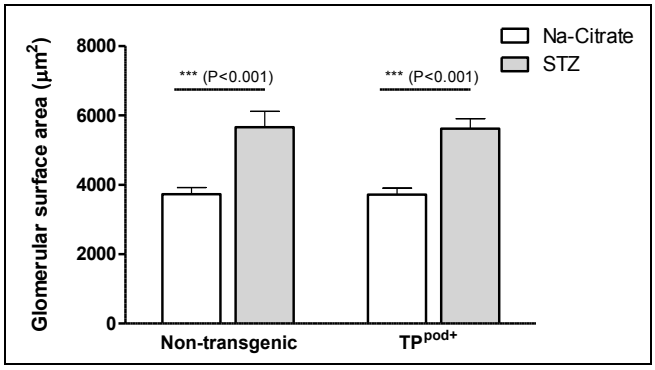

Figure 20: Medium dose of STZ induces minor renal and glomerular pathology.

The average of each kidney weights has been normalized to each mouse body weight measured by ACVS personal on the morning of sacrifice (A). 4µm paraffin sections of kidney samples fixed for 24 hours in 4% paraformaldehyde were stained by periodic acid-Schiff (PAS). Representative pictures (B, 1: non-transgenic Na-Citrate, 2: non-transgenic STZ, 3: TP^{pod+} Na-Citrate, 4: TP^{pod+} STZ) were taken and glomerular diameter of 20 glomeruli per mouse was measured using Zeiss Axiovision Rel 4.8 in a blinded manner (C). The statistical analysis was done using two-way ANOVA in GraphPad Prism.

A.

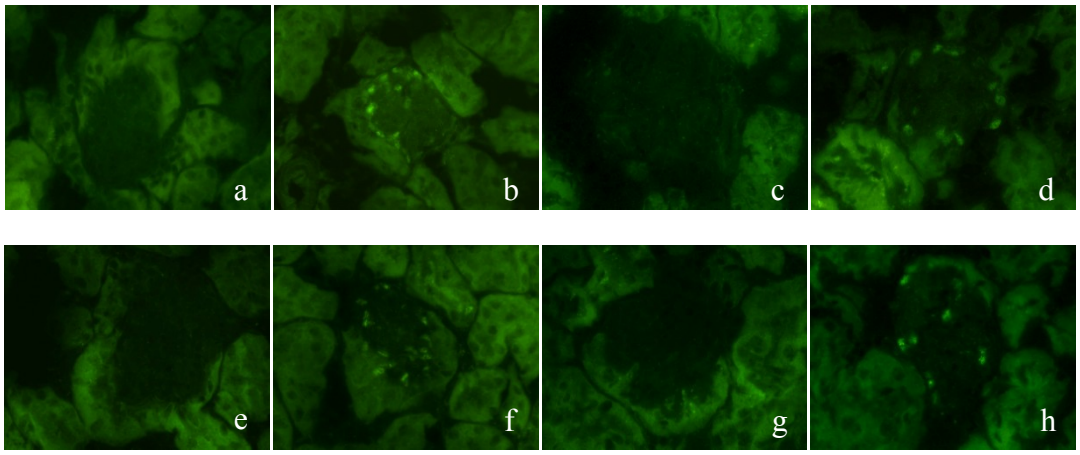

B.

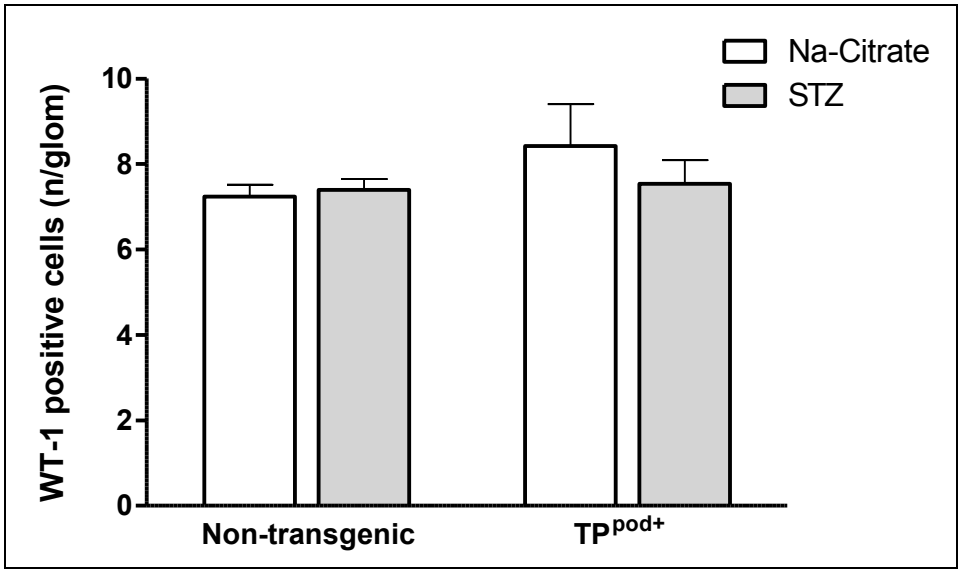

Figure 21: Medium dose of STZ tend to induce podocyte loss.

8µm frozen sections of kidney samples embedded in O.C.T. were stained for detection of Wilm's tumor 1 (WT-1) and analyzed using Zeiss Axioskop 2 fluorescence microscope. A. Representative pictures illustrate all different conditions (b: non-transgenic Na-Citrate injected, d: non-transgenic STZ-injected, f: TP^{pod+} Na-Citrate injected, h: TP^{pod+} STZ-injected) and their controls (a,c,e,g: staining without primary antibody against WT-1). B. The analysis was done in a blinded manner using Zeiss Axiovision Rel 4.8 to determine the average of WT-1 positive cells per glomeruli, over 20 glomeruli per mouse. The statistical analysis was done using two-way ANOVA in GraphPad Prism.

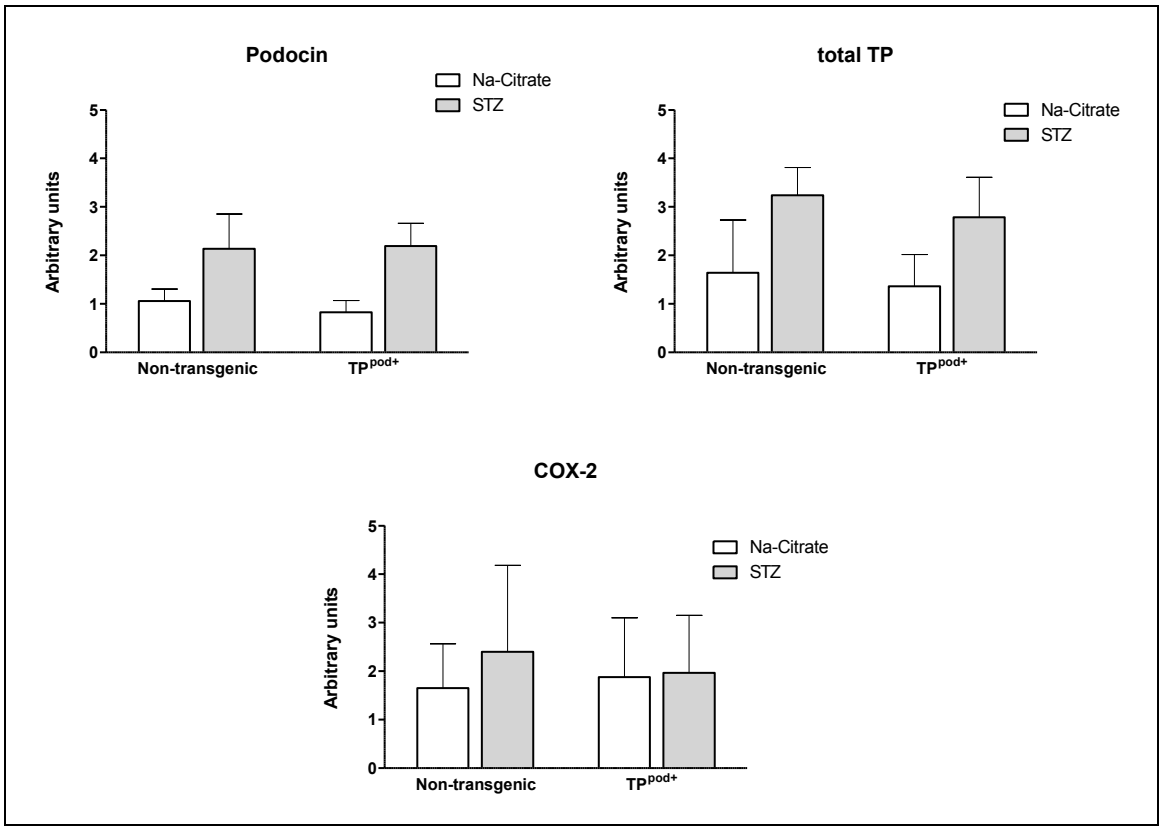

Figure 22: Podocin, total TP and COX-2 cortical mRNA expression.

RNA was extracted from approximately 20mg of snap frozen cortex as described in materials and methods and 1µg was reverse transcribed before analysis by quantitative PCR. Primers for podocin, total TP, and COX-2 were used as well as β-actin as a reaction control. Each primer set was normalized to its reaction control β-actin before being normalized again to the average of Na-Citrate non-transgenic mice. Arbitrary units are determined by calculation of $2^{-\Delta\Delta Ct}$. Statistical analysis was done using two-way ANOVA in GraphPad Prism.

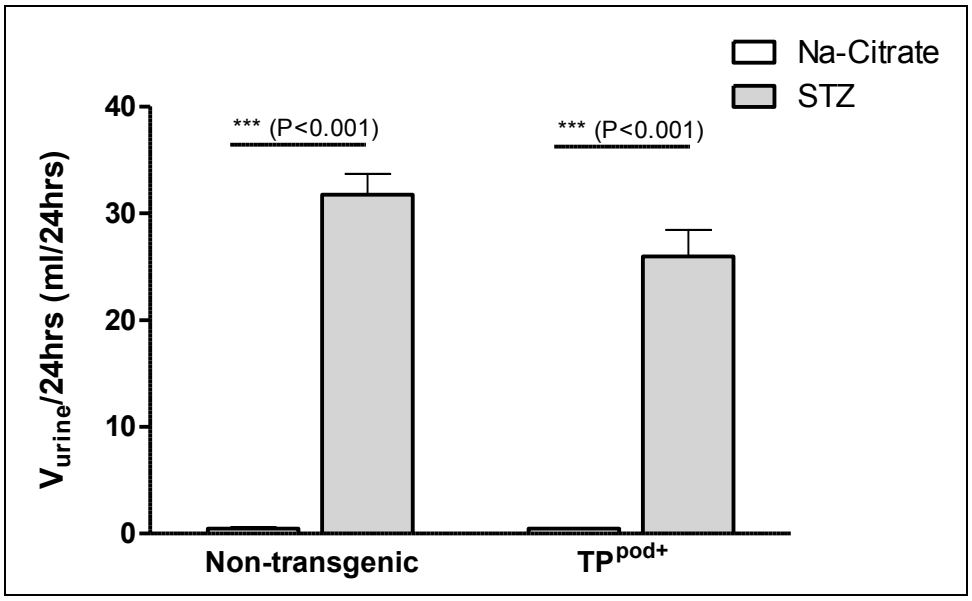

Figure 23: Type-1 diabetes induces polyuria in medium STZ dose injected mice.

At eight weeks post-injections, mice were placed into metabolic cages for 24 hours. Urine was collected and the volume obtained was measured. Statistical analysis of the data was done using two-way ANOVA in GraphPad Prism.

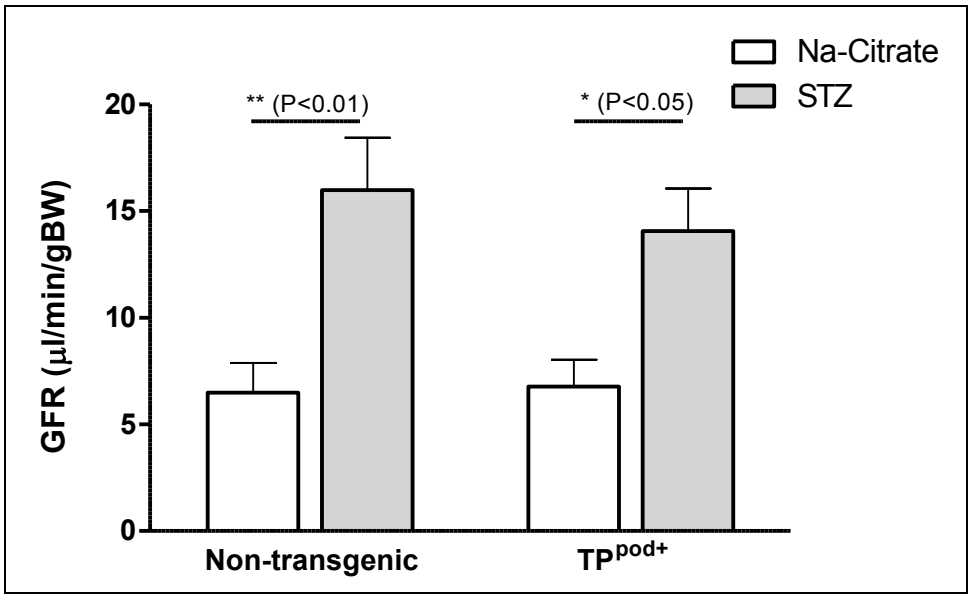

Figure 24: Medium dose of STZ induces a glomerular filtration rate increase.

A saphenous vein injection of 5% FITC-inulin solution (dose of 3.74µl/gBW) followed by blood collection between 3 and 75min post-injection helped to determine the disappearance of inulin in the plasma and calculate the glomerular filtration rate (GFR) using a two-compartment clearance model in GraphPad Prism followed by a statistical two-way ANOVA.

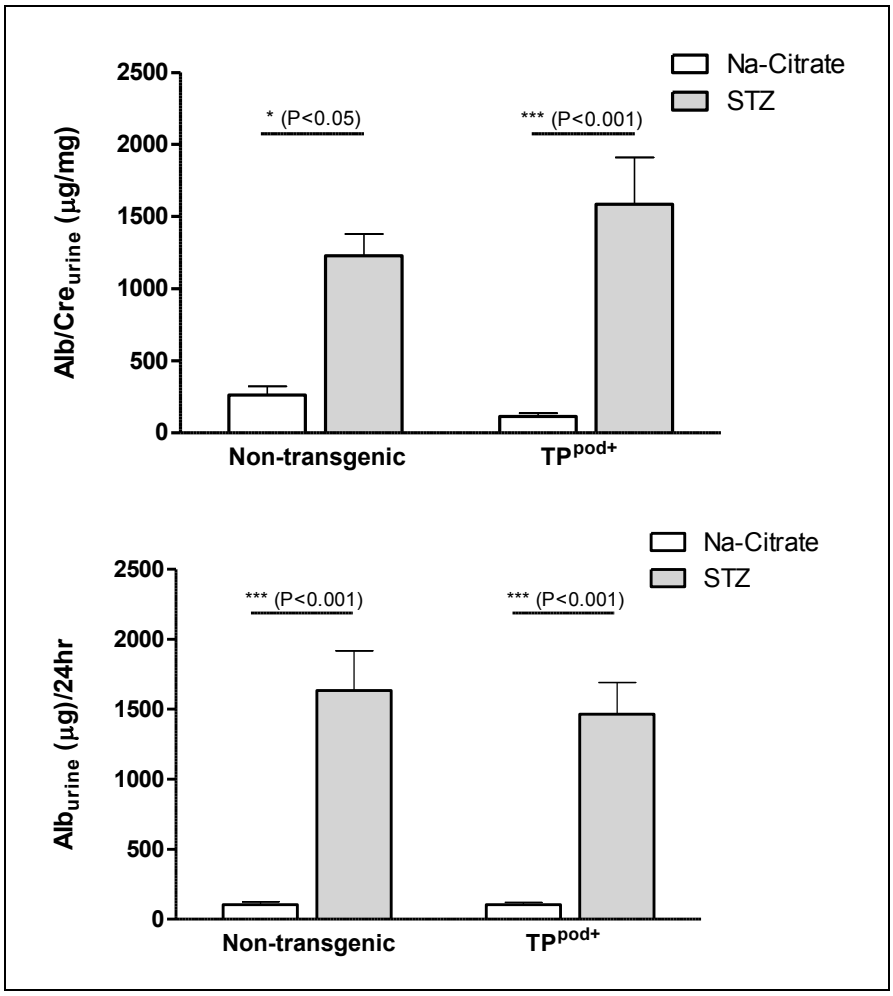

Figure 25: Medium dose of STZ induces glomerular filtration barrier damages.

24 hour urine collection samples were submitted to albumin quantification using the Mouse Albumin ELISA Kit (Bethyl Laboratories Inc.) and have been normalized to creatinine concentration (measured by Creatinine Companion ELISA kit, Exocell; top panel) or to 24 hour volume (bottom panel).

Chapter IV: Discussion

1. The effects of TP antagonist administration on glomerular filtration barrier integrity in the STZ type-1 diabetic mouse model

In order to investigate whether TXA_2/TP receptor signalling is involved in the glomerular filtration barrier damage observed in diabetic nephropathy, we treated STZ-induced type-1 diabetic mice with chronic infusions of the TP receptor antagonist SQ29548 over a 4 week period.

In 1985, Ogletree, Harris *et al.* described the pharmacological antagonist activity of SQ29548 as selective for the TP receptor. This antagonist prevented platelet aggregation, tracheal spirals, and aortic strip contractions in response to several TP agonists without influencing thromboxane synthase activity or other prostanoid pathways (Ogletree, Harris *et al.* 1985). More recently, Shineman, Zhang *et al.* demonstrated the involvement of the TP receptor in the progression of Alzheimer's disease. Administration of TP antagonists, SQ29548 through osmotic mini-pumps or S18886 via drinking water, prevented amyloid plaque development *in vivo* in a similar manner. *In vitro*, both treatments presented comparable blockade of increased signalling molecules involved in this pathological process (Shineman, Zhang *et al.* 2008).

To date, no studies involving SQ29548 delivered by osmotic mini-pump in diabetic models have been reported. However, administration of the TP receptor antagonist

S18886 in the drinking water was found to provide a renoprotective effect in models of type-1 and type-2 diabetes. In both models, the authors observed protection against histological glomerular and tubular damages as well as a reduction of oxidative stress products and markers of renal impairment including polyuria and proteinuria (Xu, Jiang *et al.* 2006; Sebekova, Eifert *et al.* 2007).

Furthermore, treatment with FCE 22178, a specific thromboxane synthase inhibitor, in a model of renal mass reduction resulted in similar effects to those obtained with TP antagonists along with an increase in urinary PGI_2 products (Zoja, Perico *et al.* 1990). The same study demonstrated a decrease in systemic blood pressure, which the authors associated with a vasodilatory PGI_2 effect on peripheral vascular resistance suggesting that TP signalling normally acts to limit prostacyclin production or signalling (Zoja, Perico *et al.* 1990).

Interestingly, treatment of type-1 diabetic rats with both a thromboxane synthase inhibitor (4'(imidazol-l-yl) acetophenone) and a TP antagonist (Bay U3405) did not ameliorate proteinuria more than treatment with only the thromboxane synthase inhibitor. This finding suggests that the thromboxane synthase inhibitor is sufficient to ablate TP ligand levels and effectively attenuate TP signalling (Craven, Melhem *et al.* 1992).

Technical limitations (solubility of the compound and osmotic mini-pumps model adapted for mouse) prevented us from administering the TP receptor antagonist,

SQ29548, at a dosage of 2mg/kg/day as was previously reported by both Sebekova, Eifert *et al.*, and Xu, Jiang *et al.* However, our treatment with 660µg/kg/day was sufficient to effectively prevent a number of characteristic features of diabetic nephropathy such as absence of significant kidney and glomerular hypertrophy, prevention of polyuria and albuminuria, and a significant conservation of podocyte numbers per glomerulus.

The correlation between podocyte loss and proteinuria is stronger for type-1 diabetic mice models than for type-2 models. In both models, this association is supported by increased podocyte apoptosis at an early stage of the disease. This phenomenon was shown to be glucose-related by *in vitro* exposure of mouse podocytes to increasing concentrations of glucose (Susztak, Raff *et al.* 2006). However, podocyte loss can also be attributed to detachment from the glomerular basement membrane due to reduced levels of integrins in diabetes (Chen, Chen *et al.* 2000). Podocytes (characterized as nephrin, podocin, synaptopodin, WT-1 positive cells) isolated from urine of experimental models of glomerulopathy were viable for up to 72 hours *ex vivo* (Petermann, Krofft et al. 2003; Petermann, Pippin et al. 2004).

Due to the impact of blood pressure on glomerular hemodynamic parameters, current treatments for diabetic patients include blood pressure regulators such as angiotensin converting enzyme inhibitors or angiotensin receptor blockers. Similar treatments administrated to diabetic mice (perindopril) were able to reduce the appearance of proteinuria (Kelly, Aaltonen *et al.* 2002). The renin-angiotensin system is implicated in

the regulation of systemic as well as renal hemodynamics. The latter involves an increase in renal vasculature resistance, specifically at the efferent arteriole location. The activation of this mechanism in diabetes might be due to hyperglycemia (Arima & Ito 2003). However, the appearance of increased systemic blood pressure in a model of low dose STZ diabetes was demonstrated after 15 to 30 weeks of diabetes (Breyer, Bottinger *et al.* 2005). It is, therefore, not surprising that no blood pressure variation was observed over a 4 week period. The lack of effect of the TP antagonist on systemic blood pressure indicates that the vasoconstrictor effect of the TP receptor is not as highly implicated in blood pressure management as other blood pressure regulatory systems (e.g., the renin-angiotensin system). The decrease in systemic blood pressure observed during a global inhibition of thromboxane A_2 synthesis was potentially due to an increase in vasodilatory PGI_2 production (Zoja, Perico *et al.* 1990).

Systemic blood pressure changes do not necessarily translate into alterations in glomerular hemodynamics. Two mechanisms protect the glomerulus against a rise in systemic blood pressure: 1) the myogenic response in which preglomerular vasoconstriction occurs in response to increased vascular stretch due to rising systemic blood pressure and 2) tubuloglomerular feedback in which vasoconstriction of the afferent arteriole occurs in response to ionic (NaCl) tubular fluids composition fluctuation sensed by the macula densa (part of the thick ascending limb directly interacting with both afferent and efferent arterioles forming the juxtaglomerular apparatus) (Arima & Ito 2003; Koeppen & Stanton 2007). However, a simultaneous vasodilation of the afferent

arteriole due to hyperglycemia (increased glucose reabsorption, decreased sodium concentration in tubules, macula densa increased prostanoids production) and vasoconstriction of the efferent arteriole, in part through TP receptor activation, may lead to increased glomerular capillary pressure resulting in higher glomerular filtration rate and renal plasma flow. The stretch and the increased level of filtration are likely injurious to the glomerular filtration barrier due to podocyte cytoskeleton remodelling (Hayashi, Epstein *et al.* 1992; Arima & Ito 2003).

The presence of transcription factor binding sites in the promoter region of the COX-2 gene allows the rapid production of COX-2 in response to pathophysiological conditions such as diabetes. Its presence in the renal vasculature, the medullary interstitial cells, and the macula densa plays an important role in the regulation of hemodynamic parameters (Hinz & Brune 2002). In experimental diabetes, cortical COX-2 was elevated (Komers, Lindsley *et al.* 2001) and glomerular COX-2 mRNA expression was increased in response to various types of kidney disease (diabetic nephropathy, minimal change disease) (Cheng, Wang *et al.* 2007). In podocytes, both mRNA and protein levels were increased in response to mechanical stretch (Martineau, McVeigh *et al.* 2004). In our studies, the absence of COX-2 mRNA upregulation in the renal cortex of diabetic mice was surprising. We speculate that the time frame of 4 weeks of diabetes was insufficient to allow the development of high level of inflammation in the kidney cortex. Further analysis at the glomerular level could also reveal more subtle changes.

Similar observations apply to TP mRNA expression. Cultured mouse podocytes exposed to diabetic conditions (high glucose, mechanical stretch) expressed higher mRNA levels of the TP receptor (Shaji 2011). Cortical mRNA expression of the TP receptor showed a non-statistically significant upward trend in diabetic mice. Since TP receptor expression is responsive to its own stimulation by its ligand, and thromboxane A_2 is formed in part through the enzymatic actions of COX-2, it is plausible that similarly to COX-2, the TP receptor mRNA variation was localized to the glomeruli and its induction was masked by dilution due to other cell types in the cortex

Markers of slit diaphragm damage were analysed at the transcriptional level. The absence of decreased nephrin mRNA expression is not surprising after only 4 weeks of diabetes. In their study, Kelly, Aaltonen *et al.* could not detect any change in glomerular nephrin expression in short term type-1 diabetes; whereas, a significant decrease was observed in a long term study (Kelly, Aaltonen *et al.* 2002). However, the marked increase in nephrin and podocin mRNA expression in diabetic mice infused with the TP antagonist is intriguing.

Most kidney diseases such as diabetic nephropathy are associated with a down regulation of nephrin mRNA and protein expression (Chen, Stead *et al.* 2012; Lee, Kim *et al.* 2012; Nadarajah, Milagres *et al.* 2012) which are associated with podocyte loss and proteinuria. Those findings were confirmed in clinical studies showing a correlation between the urinary nephrin level (nephrinuria) and the degree of proteinuria due to diabetes (Patari,

Forsblom *et al.* 2003; Jim, Ghanta *et al.* 2012). In the Akita mice model of type-1 diabetes, Chang, Paik *et al.* demonstrated that there is an association between increased urinary nephrin expression and podocyte apoptosis before the appearance of significant albuminuria at 4 week of age (Chang, Paik *et al.* 2012). These clinical and experimental data suggest that the appearance of nephrin in urine could be an early marker of slit diaphragm damage.

PPARs are nuclear receptor proteins acting as transcription factors. They have been linked to the regulation of many cellular events including differentiation, proliferation, survival, and inflammation. Most importantly, PPARs have the ability to induce slit diaphragm gene expression including nephrin and synaptopodin (Miglio, Rosa *et al.* 2011), and their renal mRNA expression is similarly decreased along with slit diaphragm components in models of type-1 diabetes (Proctor, Jiang *et al.* 2006). Mouse podocytes were protected against hyperglycemia-induced nephrin downregulation by treatment with a PPARδ agonist. Similarly, nephrin mRNA and protein levels were restored in diabetic patients treated with a specific agonist of PPARδ. Furthermore, significant decreases in glomerular basement membrane thickening and albuminuria were observed in these patients (Lee, Kim *et al.* 2012). Importantly, prostacyclin (the endogenous ligand of the IP receptor) activation of PPARβ leaded to vasodilatation and reduced thrombosis (Hao, Redha *et al.* 2002; Mitchell, Ali *et al.* 2008), whereas PPARγ regulated TP and TXA_2 mRNA expression (Coyle, O'Keeffe *et al.* 2005). Taken together, it remains possible that TP antagonism by SQ29548 allows free prostacyclin signalling that promote

nephrin/podocin induction in a PPAR-dependent manner. Further work will be necessary to verify this hypothesis.

In summary, mice injected with STZ developed type-1 diabetes and infusion of the thromboxane receptor antagonist appears to not only prevent early signs of diabetic nephropathy such as glomerular hypertrophy and podocyte loss but also to reduce the impact of diabetes on kidney function by preventing hyperfiltration and damage to the glomerular filtration barrier. With the demonstration of a role for TXA_2/TP signalling in the progression of diabetic nephropathy, future work will undoubtedly be focussed on identifying the cellular target of this pathway that underlies glomerular filtration barrier damage and albuminuria.

2. Podocyte-specific thromboxane receptor overexpression in STZ type-1 diabetes mice.

As discussed above, results of our antagonist study demonstrated a significantly slower disease development which concurs with the literature and indicated an important role for the TXA_2/TP receptor signalling in diabetic nephropathy (Figure 26). The specific cellular location of such deleterious TXA_2/TP receptor signalling remained undetermined. Previous experiments in our laboratory demonstrated an increase in TP receptor mRNA expression and TXA_2 release by mouse podocytes exposed to diabetic conditions (high glucose and mechanical stretch). The same podocyte undergo apoptosis when exposed to TP agonist U46619 (Shaji 2011). We hypothesized that the podocyte was a reasonable target and, therefore, generated mice with podocyte-specific TP overexpression with the idea that filtration barrier damage in TP^{pod+} mice would be exacerbated in response to STZ-induced diabetes.

However, TP^{pod+} and the non-transgenic mice showed similar responses to STZ treatment with no significant differences observed for any of the parameters analysed including albuminuria (Figure 26). These findings are consistent with at least three possibilities:

1) Transgenic TP expression was not greater than endogenous receptor levels in diabetic mice

2) Despite adequate expression, the transgenic receptor was not sufficiently functional and, therefore, thromboxane-mediated signalling was severely limited
3) Transgenic TP expression and signalling were robust but the pathophysiological effects of TXA_2/TP receptor activation reside in cellular locales other than the podocyte.

1) Characterization of the transgenic mouse line by Ms. Shaji demonstrated a significant increase in mRNA expression within the kidney and immunofluoresence staining against the HA-tag located HA-TP to the glomerulus (Shaji 2011). Quantitative PCR analysis of total TP in the kidney cortex indicated a slight increase in total TP mRNA expression in STZ-induced diabetes which is also concurrent with the literature. However, total TP mRNA expression in TP^{pod+} diabetic was no greater than that of non-transgenic mice. It remains possible that variations in podocyte mRNA levels of TP receptor are hidden by the large variety of other cell types within the cortex. Therefore it will be recommended to further investigate TP receptor mRNA expression at the glomerular level. Extraction of glomeruli out of frozen sections by laser micro-capture is one technique currently available to us.

An overexpression of a receptor does not imply that its ligand will be produce. It has been reported in the literature, as well as in our lab (Kennedy lab, unpublished, (Shaji 2011), that podocytes are able to produce thromboxane A_2 which can be measured under its stable metabolite form thromboxane B_2 in the cell culture media (Craven, Melhem *et al.*

1992; Sebekova, Eifert *et al.* 2007; Shaji 2011). A measure of the levels of this metabolite could in fact insure that both ligand and receptor were present and enhanced in urine of diabetic mice. Since both TP and TXA_2 production are reported to be enhanced in diabetic kidneys, it is possible that overexpressing TP reaches the maximum level of TP signalling allowed by the cell at baseline, and this signalling pathway will not be further stimulated even in pathological situations. However, since kidney or glomerular injury were not observed in non-diabetic TP^{pod+} mice, it is possible that the endogenous TP receptor is desensitized to offset signalling induced by transgenic TP expression. The assessment of this mechanism could be performed by quantitative PCR. Despite our intention to differentially measure the expression level of total TP and compare it to the expression level of transgene, several primer sets designed against the HA tag of the transgenic TP failed to amplify a unique product.

2) Our studies aimed at verifying the activity of the overexpressed TP receptor were inconclusive. Both of the markers selected from the results of a micro-array chip study previously carried out (Kennedy lab, unpublished) did not respond to stimulation with the TP agonist. The absence of statistically significant results could have been derived from the variation in methodology. Samples tested by micro-array were the result of *in vitro* stimulation of mouse podocytes whereas the results presented here are from stimulation of isolated glomeruli. Therefore, it is possible that the different cell types within the glomerulus may have diluted the effect of the TP agonist on gene transcription. Glomerular calcium influx assays with the TP agonist showed some indications of

responsiveness by the TP^{pod+} versus non-transgenic mice. However, there were reproducibility issues between glomeruli of the same mouse in these experiments which suggests that either experimental conditions were suboptimal or transgene expression was highly variable within the same mouse.

3) Since TP activity has been mainly observed in platelets and in the vasculature, it is possible that the protective effect of a specific TP antagonist on diabetic nephropathy development is not directly related to the activity of podocyte TP populations. This receptor has been localized in many cell types of the kidney such as smooth muscle cells of renal efferent and afferent arterioles, proximal tubular cells, mesangial cells, and within the thick ascending limb and distal convoluted tubules (Abe, Takeuchi *et al.* 1995; Bresnahan, Le Breton *et al.* 1996; Breyer & Breyer 2001; Huang, Ramamurthy *et al.* 2004). Increased production of TXA_2 could in fact lead to efferent arteriole contraction to reduce renal blood flow and increase filtration fraction which would expose the glomerular filtration barrier, including its podocytes, to aberrantly high mechanical forces thereby promoting albuminuria (Figure 27). Despite intriguing features of the $TP^{-/-}$ mice (i.e., increased renal vascular resistance and reduced renal blood flow) that the authors attributed to a developmental defect, the decrease in systemic blood pressure and renal blood flow along with enhanced oxidative stress in angiotensin-II chronically infused mice, indicates mediation of the AT_1 receptor (angiotensin-II receptor, type 1) signalling through TP receptor activation. As renal angiotensin II levels are elevated during diabetes,

arteriolar TP receptors may therefore indirectly promote albuminuria from outside of the glomerular filtration barrier (Kawada, Dennehy *et al.* 2004).

Interestingly, it has to be considered that the TP receptor is not only activated by TXA_2. The actions of PGH_2 as well as isoprostanes, non-enzymatic products of the arachidonic acid pathway, were suppressed by co-incubation with TP antagonists. Production of isoprostane is enhanced with oxidative stress conditions found in diabetic nephropathy and acts mainly on the renal vasculature to increase preglomerular vasculature resistance which then reduces glomerular filtration rate and renal blood flow (Badr & Abi-Antoun 2005) (Figure 27).

On the other hand, stimulation of mesangial cells with a TP agonist resulted in contraction and proliferation along with production of extracellular matrix components (collagen, fibronectin, laminin) and transforming growth factor TGF-β (Nakahata 2008). However, a role for mesangial TP populations is unlikely since matrix production is not positively correlated with albuminuria levels in diabetes.

Lastly, TXA_2 is produced by COX-1 activity in platelets and can be interpreted as a response mechanism to systemic changes such as hyperglycemia. Vascular and glomerular cells respond to this stimulus by generating signals within the macula densa, the main COX-2 production centre, to synthesize additional prostanoids to restore an equilibrium between vasoconstrictor/dilators (Nasrallah, Clark *et al.* 2007). It has been

demonstrated that in STZ-induced type-1 diabetes, the ratio of PGI_2/TXA_2 is reduced due to an increased production of TXA_2 as well as a decreased production of PGI_2. This unbalance was corrected with high ingestion of Vitamin E (Kwag, Kim *et al.* 2001).

In summary, TP receptor is the target of enzymatic and non enzymatic products to act as a vasoconstrictor on the renal but not systemic vasculature (Figure 27). It also mediates oxidative stress and inflammation and promotes extracellular matrix production under diabetic conditions. However those properties might not be linked to the podocyte itself.

3. Conclusions

This study demonstrated a positive effect of a low dose of TP antagonist to delay the progression of diabetic nephropathy. A potential involvement of PPAR was hypothesized due to higher level of nephrin mRNA expression in the cortex. However, overexpression of the TP receptor in podocytes failed to demonstrate an implication of those cells in diabetic nephropathy progression. Functional characterization of the receptor was unsuccessful and remains to be completed in order to validate the results (Figure 26).

The goal of this project was to identify a pharmacological target involved in diabetic nephropathy that would allow for more specific attenuation of filtration barrier injury while bypassing the adverse side-effects of NSAIDs and Coxibs. Despite the fact that podocytes appear to not be directly implicated, significant work remains to identify the source of TXA_2/TP signalling effects in this particular disease.

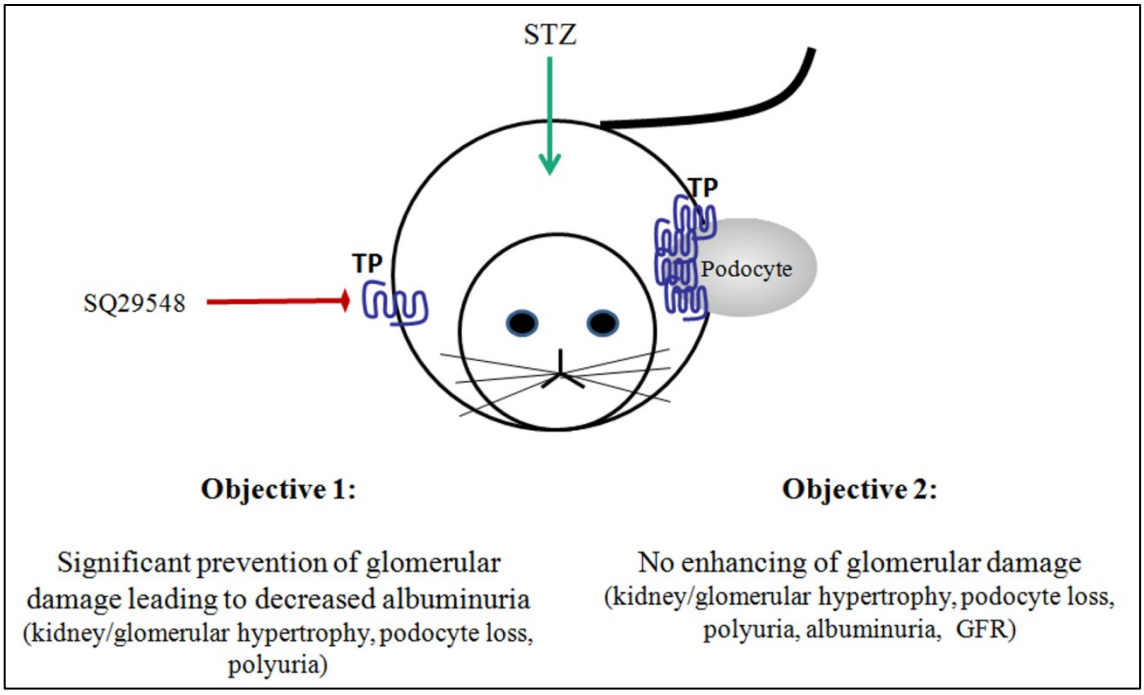

Figure 26: Schematic summary of experimental findings.

In the objective 1 (left panel), diabetic and non-diabetic mice were infused with 660µg/kg/day of SQ29548, a TP antagonist. After 4 weeks of diabetes, a significant prevention of glomerular damage was observed along with a decreased in albuminuria. However, the overexpression of the TP receptor in podocytes did not enhanced the glomerular damages seen in non-transgenic mice, after 11 weeks of diabetes (right panel).

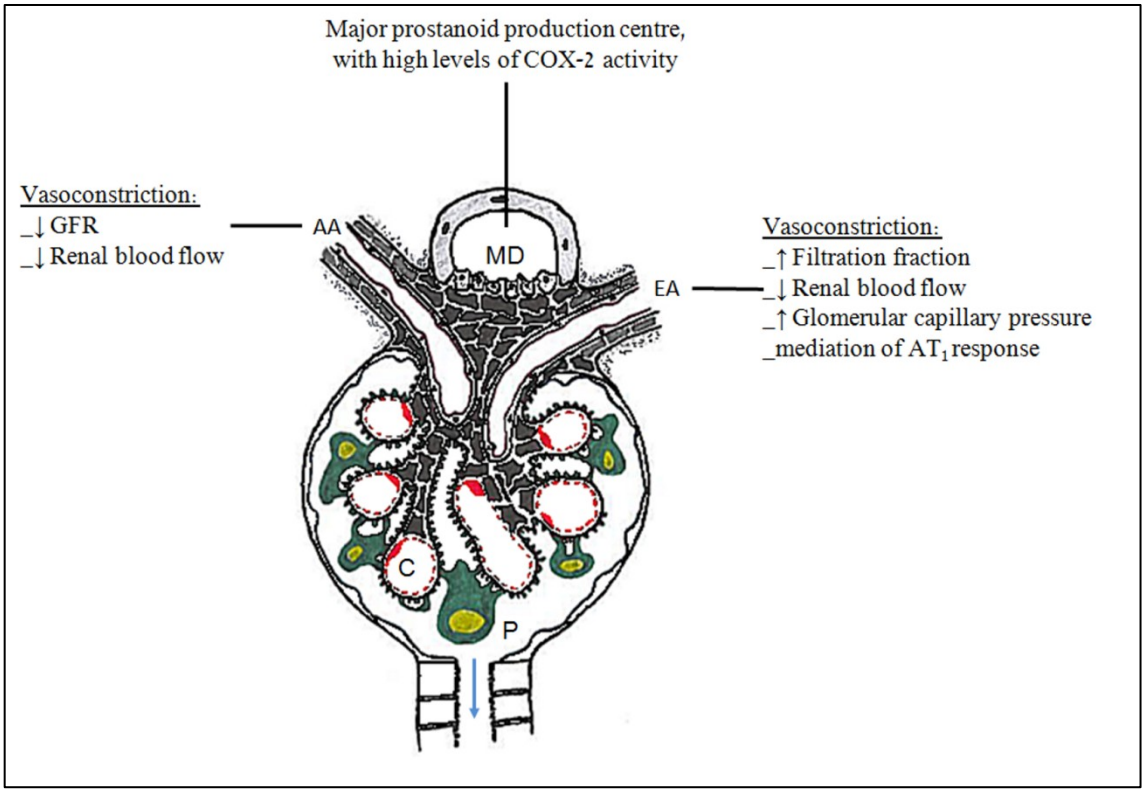

Figure 27: Glomerular thromboxane A_2 responsive sites influencing albuminuria in diabetic nephropathy.

Thromboxane A_2, produced by COX-2 in the macula densa (MD) or COX-1 in platelets, induces vasoconstriction of the afferent arteriole (AA) leading to decreased glomerular filtration rate (GFR) and renal blood flow. Stimulation of TP receptors in the efferent arteriole (EA) by thromboxane A_2 leads to vasoconstriction of the vessel. Despite a similar decline in renal blood flow, post-glomerular vasoconstriction raises glomerular capillary pressure and filtration fraction. TP receptors in the efferent arteriole mediate the response to angiotensin-II stimulation.

References

(IDF), I. D. F. (2009). "Diabetes Atlas." 4. Retrieved March 2011, from http://www.diabetesatlas.org/.

Abe, T., Takeuchi, K., *et al.* (1995). "Rat kidney thromboxane receptor: molecular cloning, signal transduction, and intrarenal expression localization." J Clin Invest **96**(2): 657-64.

Arima, S. & Ito, S. (2003). "The mechanisms underlying altered vascular resistance of glomerular afferent and efferent arterioles in diabetic nephropathy." Nephrol Dial Transplant **18**(10): 1966-9.

Ayodele, O. E., Alebiosu, C. O., *et al.* (2004). "Diabetic nephropathy--a review of the natural history, burden, risk factors and treatment." J Natl Med Assoc **96**(11): 1445-54.

Badr, K. F. & Abi-Antoun, T. E. (2005). "Isoprostanes and the kidney." Antioxid Redox Signal **7**(1-2): 236-43.

Bek, M., Nusing, R., *et al.* (1999). "Characterization of prostanoid receptors in podocytes." J Am Soc Nephrol **10**(10): 2084-93.

Bresnahan, B. A., Le Breton, G. C., *et al.* (1996). "Localization of authentic thromboxane A2/prostaglandin H2 receptor in the rat kidney." Kidney Int **49**(5): 1207-13.

Breyer, M. D., Bottinger, E., *et al.* (2005). "Mouse models of diabetic nephropathy." J Am Soc Nephrol **16**(1): 27-45.

Breyer, M. D. & Breyer, R. M. (2001). "G protein-coupled prostanoid receptors and the kidney." Annu Rev Physiol **63**: 579-605.

Burgess, E. (2008). "Slowing the progression of kidney disease in patients with diabetes." J Am Soc Hypertens **2**(4 Suppl): S30-7.

Cathcart, M. C., Reynolds, J. V., *et al.* (2010). "The role of prostacyclin synthase and thromboxane synthase signaling in the development and progression of cancer." Biochim Biophys Acta **1805**(2): 153-66.

Chang, J. H., Paik, S. Y., *et al.* (2012). "Diabetic kidney disease in FVB/NJ Akita mice: temporal pattern of kidney injury and urinary nephrin excretion." PLoS One **7**(4): e33942.

Chang, R. L., Deen, W. M., *et al.* (1975). "Permselectivity of the glomerular capillary wall: III. Restricted transport of polyanions." Kidney Int **8**(4): 212-8.

Chang, R. L., Ueki, I. F., *et al.* (1975). "Permselectivity of the glomerular capillary wall to macromolecules. II. Experimental studies in rats using neutral dextran." Biophys J **15**(9): 887-906.

Chen, H. C., Chen, C. A., *et al.* (2000). "Altering expression of alpha3beta1 integrin on podocytes of human and rats with diabetes." Life Sci **67**(19): 2345-53.

Chen, L. H., Stead, B., *et al.* (2012). "Hyperglycemia and renal mass ablation synergistically augment albuminuria in the diabetic subtotally nephrectomized rat: implications for modeling diabetic nephropathy." Nephron Extra **2**(1): 115-24.

Cheng, H., Fan, X., *et al.* (2009). "Distinct roles for basal and induced COX-2 in podocyte injury." J Am Soc Nephrol **20**(9): 1953-62.

Cheng, H., Wang, S., *et al.* (2007). "Overexpression of cyclooxygenase-2 predisposes to podocyte injury." J Am Soc Nephrol **18**(2): 551-9.

Choudhury, D., Tuncel, M., *et al.* (2010). "Diabetic nephropathy -- a multifaceted target of new therapies." Discov Med **10**(54): 406-15.

Cormack-Aboud, F. C., Brinkkoetter, P. T., *et al.* (2009). "Rosuvastatin protects against podocyte apoptosis in vitro." Nephrol Dial Transplant **24**(2): 404-12.

Coyle, A. T., O'Keeffe, M. B., *et al.* (2005). "15-deoxy Delta12,14-prostaglandin J2 suppresses transcription by promoter 3 of the human thromboxane A2 receptor gene through peroxisome proliferator-activated receptor gamma in human erythroleukemia cells." FEBS J **272**(18): 4754-73.

Craven, P. A., Melhem, M. F., *et al.* (1992). "Thromboxane in the pathogenesis of glomerular injury in diabetes." Kidney Int **42**(4): 937-46.

Fanelli, F., Mauri, M., *et al.* (2011). "Light on the structure of thromboxane A(2) receptor heterodimers." Cell Mol Life Sci.

Fitzgerald, G. A. (2004). "Coxibs and cardiovascular disease." N Engl J Med **351**(17): 1709-11.

FitzGerald, G. A. & Patrono, C. (2001). "The coxibs, selective inhibitors of cyclooxygenase-2." N Engl J Med **345**(6): 433-42.

Greka, A. & Mundel, P. (2012). "Cell biology and pathology of podocytes." Annu Rev Physiol **74**: 299-323.

Gurley, S. B., Clare, S. E.*, et al.* (2006). "Impact of genetic background on nephropathy in diabetic mice." American Journal of Physiology - Renal Physiology **290**(1): F214-F222.

Hamberg, M., Svensson, J.*, et al.* (1975). "Thromboxanes: a new group of biologically active compounds derived from prostaglandin endoperoxides." Proc Natl Acad Sci U S A **72**(8): 2994-8.

Hao, C. M., Redha, R.*, et al.* (2002). "Peroxisome proliferator-activated receptor delta activation promotes cell survival following hypertonic stress." J Biol Chem **277**(24): 21341-5.

Hayashi, K., Epstein, M.*, et al.* (1992). "Impaired myogenic responsiveness of the afferent arteriole in streptozotocin-induced diabetic rats: role of eicosanoid derangements." J Am Soc Nephrol **2**(11): 1578-86.

Helmut G. Rennke, M. D. & Bradley M. Denker, M. D. (2007). Renal Pathophysiology: The Essentials, Lippincott Williams & Wilkins.

Hinz, B. & Brune, K. (2002). "Cyclooxygenase-2--10 years later." J Pharmacol Exp Ther **300**(2): 367-75.

Huang, J. S., Ramamurthy, S. K.*, et al.* (2004). "Cell signalling through thromboxane A2 receptors." Cell Signal **16**(5): 521-33.

Jefferson, J. A., Shankland, S. J.*, et al.* (2008). Chapter 21 - Molecular Mechanisms of Proteinuria. Molecular and Genetic Basis of Renal Disease. Philadelphia, W.B. Saunders**:** 373-389.

Jefferson, J. A., Shankland, S. J.*, et al.* (2008). "Proteinuria in diabetic kidney disease: a mechanistic viewpoint." Kidney Int **74**(1): 22-36.

Jim, B., Ghanta, M.*, et al.* (2012). "Dysregulated nephrin in diabetic nephropathy of type 2 diabetes: a cross sectional study." PLoS One **7**(5): e36041.

Kalant, N. (1978). "Diabetic glomerulosclerosis: current status." Can Med Assoc J **119**(2): 146-53.

Kawada, N., Dennehy, K.*, et al.* (2004). "TP receptors regulate renal hemodynamics during angiotensin II slow pressor response." Am J Physiol Renal Physiol. 2004 Oct;287(4):F753-9. Epub 2004 Jun 22.

Kelly, D. J., Aaltonen, P.*, et al.* (2002). "Expression of the slitâ€□diaphragm protein, nephrin, in experimental diabetic nephropathy: differing effects of antiâ€□proteinuric therapies." Nephrology Dialysis Transplantation **17**(7): 1327-1332.

Kimmelstiel, P. & Wilson, C. (1936). "Intercapillary Lesions in the Glomeruli of the Kidney." Am J Pathol **12**(1): 83-98 7.

Koeppen, B. M. & Stanton, B. A. (2007). Renal physiology, Mosby Elsevier.

Komers, R., Lindsley, J. N.*, et al.* (2001). "Immunohistochemical and functional correlations of renal cyclooxygenase-2 in experimental diabetes." J Clin Invest **107**(7): 889-98.

Kriz, W., Gretz, N.*, et al.* (1998). "Progression of glomerular diseases: is the podocyte the culprit?" Kidney Int **54**(3): 687-97.

Kwag, O.-G., Kim, S.-O.*, et al.* (2001). "Vitamin E Improves Microsomal Phospholipase A2 Activity and the Arachidonic Acid Cascade in Kidney of Diabetic Rats." The Journal of Nutrition **131**(4): 1297-1301.

Lee, E. Y., Kim, G. T.*, et al.* (2012). "Peroxisome proliferator-activated receptor-delta activation ameliorates albuminuria by preventing nephrin loss and restoring podocyte integrity in Type 2 diabetes." Nephrol Dial Transplant **27**(11): 4069-79.

Lewis, E. J. & Lewis, J. B. (2004). "ACE inhibitors versus angiotensin receptor blockers in diabetic nephropathy: is there a winner?" J Am Soc Nephrol **15**(5): 1358-60.

Marcantoni, C., Ortalda, V.*, et al.* (1998). "Progression of renal failure in diabetic nephropathy." Nephrol Dial Transplant **13 Suppl 8**: 16-9.

Marshall, S. M. (2004). "Recent advances in diabetic nephropathy." Postgrad Med J **80**(949): 624-33.

Martineau, L. C., McVeigh, L. I., *et al.* (2004). "p38 MAP kinase mediates mechanically induced COX-2 and PG EP4 receptor expression in podocytes: implications for the actin cytoskeleton." Am J Physiol Renal Physiol **286**(4): F693-701.

Menzel, S. & Moeller, M. J. (2010). "Role of the podocyte in proteinuria." Pediatr Nephrol.

Miggin, S. M. & Kinsella, B. T. (1998). "Expression and tissue distribution of the mRNAs encoding the human thromboxane A2 receptor (TP) alpha and beta isoforms." Biochim Biophys Acta **1425**(3): 543-59.

Miglio, G., Rosa, A. C., *et al.* (2011). "The subtypes of peroxisome proliferator-activated receptors expressed by human podocytes and their role in decreasing podocyte injury." Br J Pharmacol **162**(1): 111-25.

Mitchell, J. A., Ali, F., *et al.* (2008). "Role of nitric oxide and prostacyclin as vasoactive hormones released by the endothelium." Exp Physiol **93**(1): 141-7.

Mogensen, C. E. (1994). "Renoprotective role of ACE inhibitors in diabetic nephropathy." Br Heart J **72**(3 Suppl): S38-45.

Nadarajah, R., Milagres, R., *et al.* (2012). "Podocyte-specific overexpression of human angiotensin-converting enzyme 2 attenuates diabetic nephropathy in mice." Kidney Int **82**(3): 292-303.

Nakahata, N. (2008). "Thromboxane A2: physiology/pathophysiology, cellular signal transduction and pharmacology." Pharmacol Ther **118**(1): 18-35.

Nasrallah, R., Clark, J., *et al.* (2007). "Prostaglandins in the kidney: developments since Y2K." Clin Sci (Lond) **113**(7): 297-311.

O'Donnell, M. P., Kasiske, B. L., *et al.* (1988). "Glomerular hemodynamic and structural alterations in experimental diabetes mellitus." FASEB J **2**(8): 2339-47.

Ogletree, M. L., Harris, D. N., *et al.* (1985). "Pharmacological actions of SQ 29,548, a novel selective thromboxane antagonist." Journal of Pharmacology and Experimental Therapeutics **234**(2): 435-41.

Pagtalunan, M. E., Miller, P. L., *et al.* (1997). "Podocyte loss and progressive glomerular injury in type II diabetes." J Clin Invest **99**(2): 342-8.

Patari, A., Forsblom, C., *et al.* (2003). "Nephrinuria in diabetic nephropathy of type 1 diabetes." Diabetes **52**(12): 2969-74.

Pavenstadt, H., Kriz, W., *et al.* (2003). "Cell biology of the glomerular podocyte." Physiol Rev **83**(1): 253-307.

Proctor, G., Jiang, T., *et al.* (2006). "Regulation of renal fatty acid and cholesterol metabolism, inflammation, and fibrosis in Akita and OVE26 mice with type 1 diabetes." Diabetes **55**(9): 2502-9.

Regoli, M. & Bendayan, M. (1997). "Alterations in the expression of the alpha 3 beta 1 integrin in certain membrane domains of the glomerular epithelial cells (podocytes) in diabetes mellitus." Diabetologia **40**(1): 15-22.

Sebekova, K., Eifert, T., *et al.* (2007). "Renal effects of S18886 (Terutroban), a TP receptor antagonist, in an experimental model of type 2 diabetes." Diabetes **56**(4): 968-74.

Shaji, R. (2011). The Role of Thromboxane A2 Receptors in Diabetic Kidney Disease. Cellular and Molecular Medicine. Ottawa, University of Ottawa. **msc**.

Shankland, S. J. (2006). "The podocyte's response to injury: role in proteinuria and glomerulosclerosis." Kidney Int **69**(12): 2131-47.

Shineman, D. W., Zhang, B., *et al.* (2008). "Thromboxane receptor activation mediates isoprostane-induced increases in amyloid pathology in Tg2576 mice." J Neurosci **28**(18): 4785-94.

Simmons, D. L. (2003). "Variants of cyclooxygenase-1 and their roles in medicine." Thromb Res **110**(5-6): 265-8.

Spurney, R. F. (1998). "Role of C-terminal serines in desensitization and phosphorylation of the mouse thromboxane receptor." J Biol Chem **273**(43): 28496-503.

Steffes, M. W., Schmidt, D., *et al.* (2001). "Glomerular cell number in normal subjects and in type 1 diabetic patients." Kidney Int **59**(6): 2104-13.

Susztak, K., Raff, A. C., *et al.* (2006). "Glucose-induced reactive oxygen species cause apoptosis of podocytes and podocyte depletion at the onset of diabetic nephropathy." Diabetes **55**(1): 225-33.

System, U. S. R. D. (2012). USRDS 2012 Annual Data Report: Atlas of Chronic Kidney Disease and End-Stage Renal Disease in the United States. Bethesda, MD, National Institutes od Health, National Institute of Diabetes and Digestive and Kidney Diseases.

van Belle, T. L., Coppieters, K. T.*, et al.* (2011). "Type 1 diabetes: etiology, immunology, and therapeutic strategies." Physiol Rev **91**(1): 79-118.

Vriesendorp, R., Donker, A. J.*, et al.* (1986). "Effects of nonsteroidal anti-inflammatory drugs on proteinuria." Am J Med **81**(2B): 84-94.

Wang, J. L., Cheng, H. F.*, et al.* (2000). "A selective cyclooxygenase-2 inhibitor decreases proteinuria and retards progressive renal injury in rats." Kidney Int **57**(6): 2334-42.

Warner, T. D. & Mitchell, J. A. (2004). "Cyclooxygenases: new forms, new inhibitors, and lessons from the clinic." FASEB J **18**(7): 790-804.

Woodward, D. F., Jones, R. L.*, et al.* "International Union of Basic and Clinical Pharmacology. LXXXIII: Classification of Prostanoid Receptors, Updating 15 Years of Progress." Pharmacological Reviews **63**(3): 471-538.

Woodward, D. F., Jones, R. L.*, et al.* (2011). "International Union of Basic and Clinical Pharmacology. LXXXIII: Classification of Prostanoid Receptors, Updating 15 Years of Progress." Pharmacol Rev **63**(3): 471-538.

Xu, J., Huang, Y.*, et al.* (2010). "FVB mouse genotype confers susceptibility to OVE26 diabetic albuminuria." Am J Physiol Renal Physiol **299**(3): F487-94.

Xu, S., Jiang, B.*, et al.* (2006). "The thromboxane receptor antagonist S18886 attenuates renal oxidant stress and proteinuria in diabetic apolipoprotein E-deficient mice." Diabetes **55**(1): 110-9.

Zatz, R. & Fujihara, C. K. (2002). "Cyclooxygenase-2 inhibitors: will they help us prevent diabetic nephropathy?" Kidney Int **62**(3): 1091-2.

Zhang, L., Brass, L. F.*, et al.* (2009). "The Gq and G12 families of heterotrimeric G proteins report functional selectivity." Mol Pharmacol **75**(1): 235-41.

Zoja, C., Perico, N.*, et al.* (1990). "Thromboxane synthesis inhibition increases renal prostacyclin and prevents renal disease progression in rats with remnant kidney." J Am Soc Nephrol **1**(5): 799-807.

Appendices

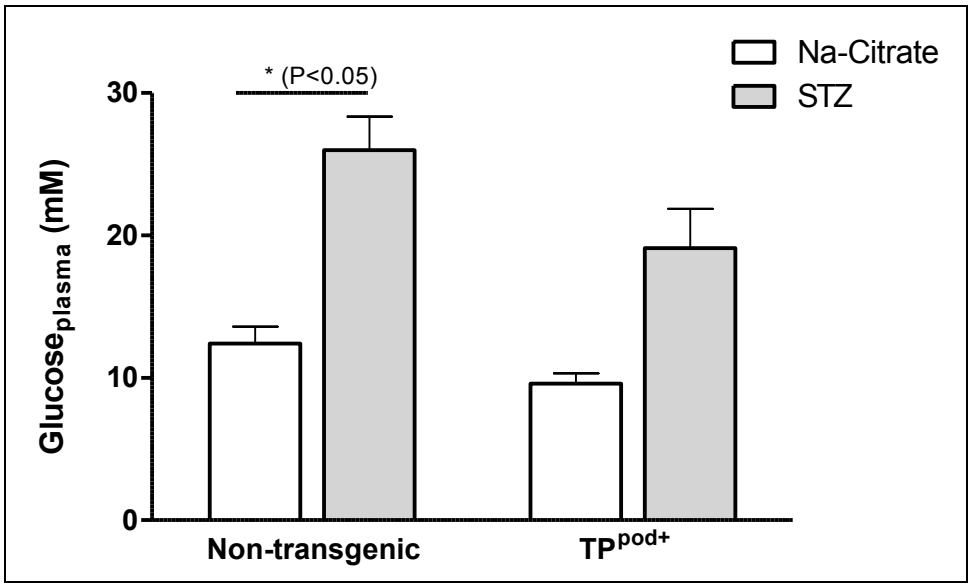

Figure 28: Plasma glucose concentration at 11 weeks post low dose STZ-injections.

Blood samples were collected at the time of sacrifice, 11 weeks post-injections, by cardiac puncture. After centrifugation (13000rpm, 20min) of the samples, plasma was isolated and conserved at -80ºC until all the samples were collected. Determination of glycemia was possible using the OneTouch Ultra2 glucometer (Lifescan Inc., Milpitas, CA). Statistical analysis was done using two-way ANOVA in GraphPad Prism. Both non-transgenic and TP^{pod+} mice injected with a low dose of STZ developed hyperglycemia with levels of 26.0 ± 2.4mM (n=5) and 19.1 ± 2.8mM (n=3) respectively versus their non-diabetic controls: 12.4 ± 1.2mM (n=2) and 9.6 ± 0.7mM (n=2) respectively.

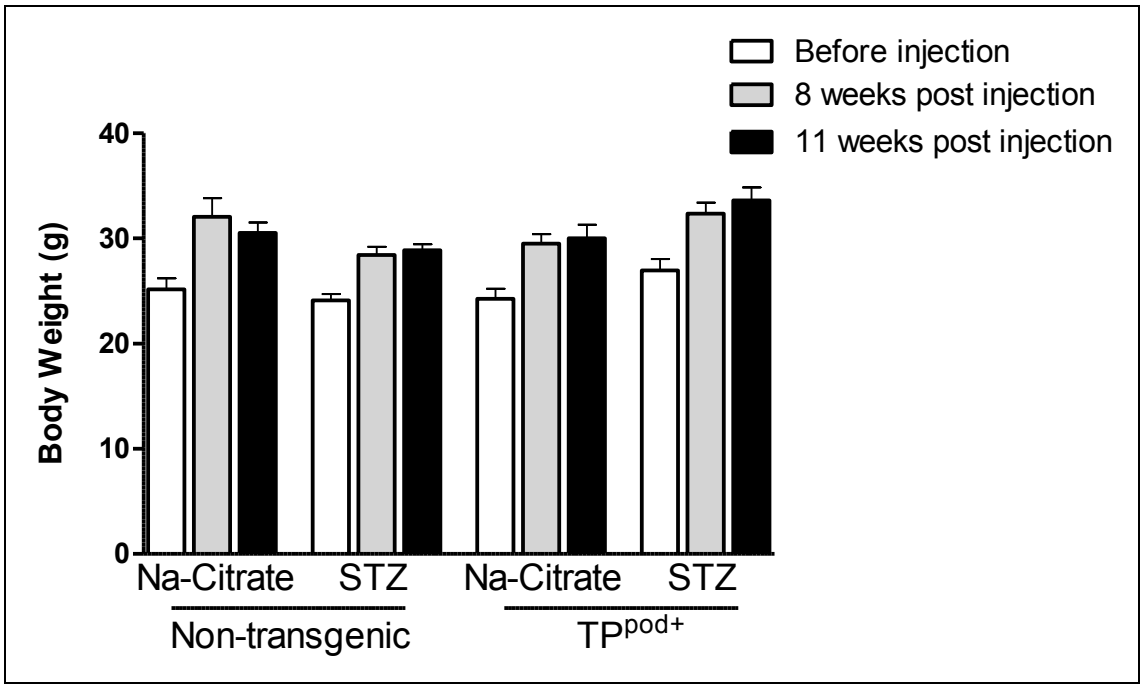

Figure 29: Body weight changes in low dose STZ injected mice.

Animal Care and Veterinarian Services of the University of Ottawa staff measured body weight on a biweekly basis. This graph illustrates a comparison of weight pre-injections, after eight weeks of diabetes (prior to metabolic cages isolation), and the morning of sacrifice (11 weeks post-injections). Statistical analysis was done using one-way ANOVA in GraphPad Prism. Both non-transgenic and TP^{pod+} STZ-injected mice gained weight throughout the 11 weeks of experiments in a similar manner: 24.1 ± 0.6g to 28.4 ± 0.8g to 28.9 ± 0.6g for non-transgenic (n=5) versus from 26.9 ± 1.1g to 32.3 ± 1.1g to 33.6 ± 1.2g for TP^{pod+} mice (n=3). Whereas non-diabetic TP^{pod+} mice follow the same trend of weight gain (24.3 ± 1.0g to 29.5 ± 0.9g to 30.0 ± 1.3g [n=2]), non-diabetic non-transgenic mice lose weight after 8 weeks (25.2 ± 1.1g to 32.1 ± 1.8g to 30.5 ± 1.0g [n=2]).

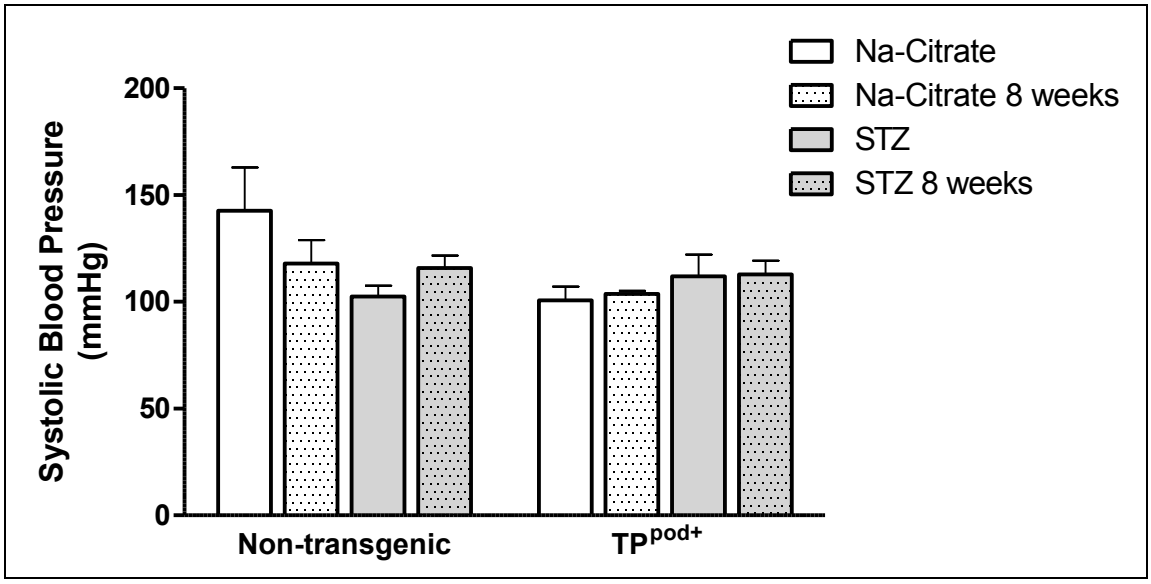

Figure 30: Blood pressure trend over 8 weeks of type-1 diabetes (STZ low dose).

Tail-cuff measurement of systolic blood pressure were done pre-injection and at 8 weeks post-injections. Statistical analysis was done using two-way ANOVA in GraphPad Prism. Variation between non-transgenic mice prior to injection (143 ± 20mmHg [*n*=2] for non-diabetic mice and 102 ± 5mmHg [*n*=5] for diabetic mice) tend to normalize at 8 weeks post-injections (118 ± 11mmHg [*n*=2] and 116 ± 6mmHg [*n*=5] respectively). On the other hand, TP^{pod+} mice tend to maintain the same values of blood pressure throughout the experiment with 101 ± 7mmHg versus 104 ± 2mmHg for the non-diabetic mice (*n*=2) and 112 ± 10mmHg versus 113 ± 6mmHg for the STZ-injected mice (*n*=3).

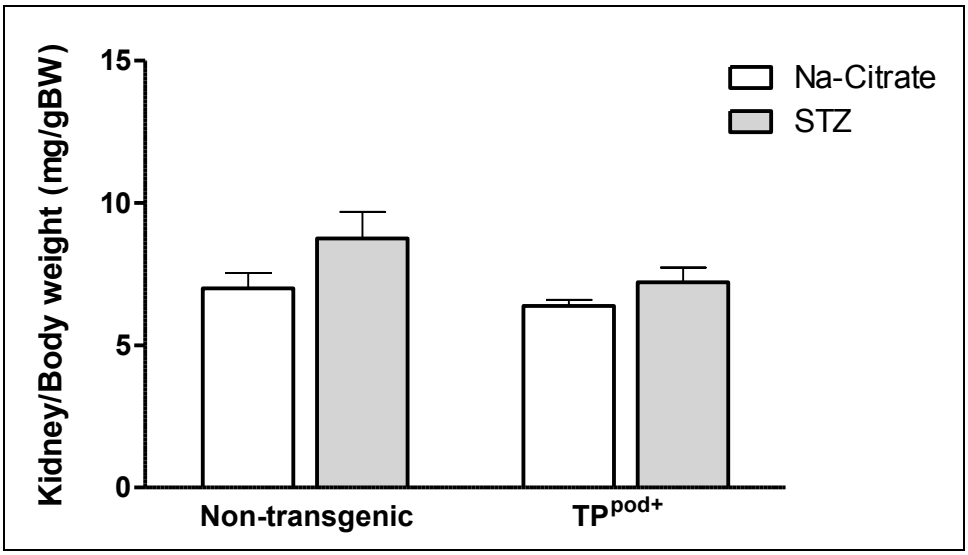

Figure 31: Diabetic mice develop kidney hypertrophy with low dose of STZ.

The average of each kidney weights has been normalized to each mouse body weight measured by ACVS personal on the morning of sacrifice. The statistical analysis was done using two-way ANOVA in GraphPad Prism. A similar mild kidney hypertrophy was noticed in both non-transgenic and TP^{pod+} STZ-injected mice: 8.8 ± 0.9mg/g (n=5) and 7.2 ± 0.5mg/g (n=3) respectively; when compared with the non-diabetic controls: 7.0 ± 0.5mg/g (n=2) and 6.4 ± 0.2mg/g (n=2) but no statistical difference was detected between non-diabetic controls and STZ-injected mice, neither between non-transgenic and TP^{pod+} mice.

A.

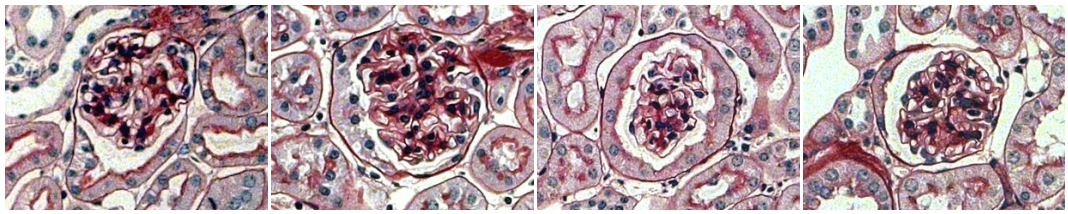

1 2 3 4

B.

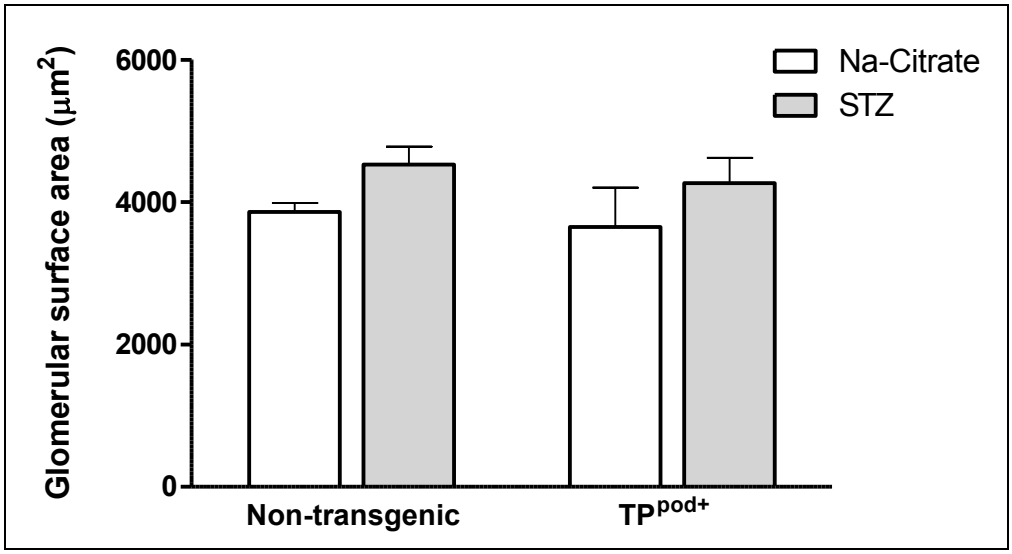

Figure 32: Minor glomerular pathology at 11 weeks post low dose STZ injection.

4µm paraffin sections of kidney samples, fixed for 24 hours in 4% paraformaldehyde, were stained by periodic acid-Schiff (PAS). Representative pictures (A, 1: non-transgenic Na-Citrate, 2: non-transgenic STZ, 3: TP^{pod+} Na-Citrate, 4: TP^{pod+} STZ) were taken and glomerular surface area of 20 glomeruli per mouse was measured using Zeiss Axiovision Rel 4.8 in a blinded manner (B). Similar observations of the ones described previously can be made. Both non-transgenic and TP^{pod+} STZ-injected mice develop glomerular hypertrophy: 4528 ± 249µm^2 (n=5) and 4265 ± 355µm^2 (n=3); when compared with their respective non-diabetic controls: 3862 ± 126µm^2 (n=2) and 3652 ± 552µm^2 (n=2) respectively. No statistical difference was detectable by two-way ANOVA in GraphPad Prism between nor non-transgenic and TP^{pod+} mice, or between Na-Citrate and STZ-injected mice in either group.

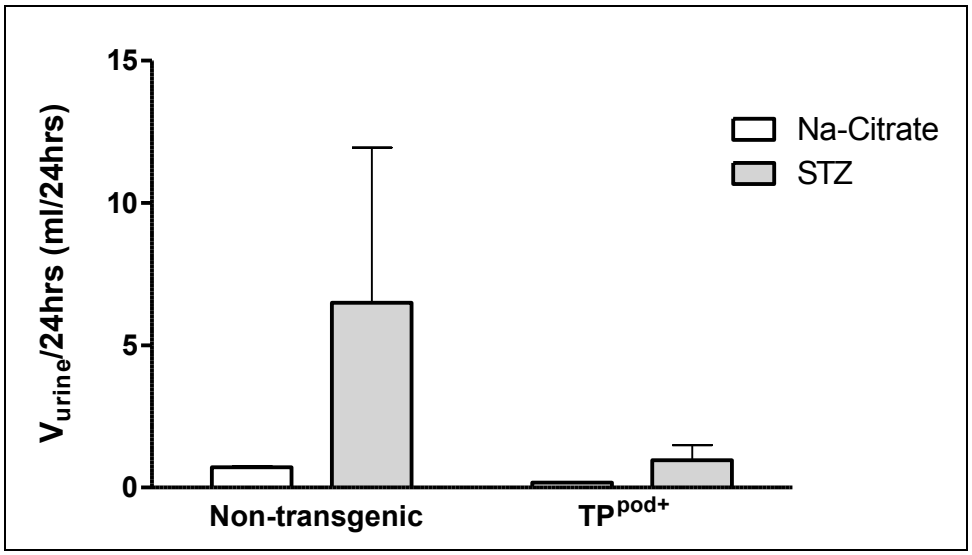

Figure 33: Low dose of STZ induces various degree of polyuria.

At eight weeks post-injections, mice were placed into metabolic cages for 24 hours. Urine was collected and the volume obtained was measured. Although non-transgenic STZ-injected mice have a tendency to develop polyuria (6.49 ± 5.45ml/24hrs [*n*=4] when compared to their non-diabetic controls 0.72 ± 0.04ml/24hrs [*n*=2]), TP^{pod+} STZ-injected mice developed a really mild polyuria with only 0.97 ± 0.52ml/24hrs (*n*=3) versus 0.17ml/24hrs for the non-diabetic control. No statistical difference has been detected in either group when compared with their control or when compared to each other. Statistical analysis was done using two-way ANOVA in GraphPad Prism.

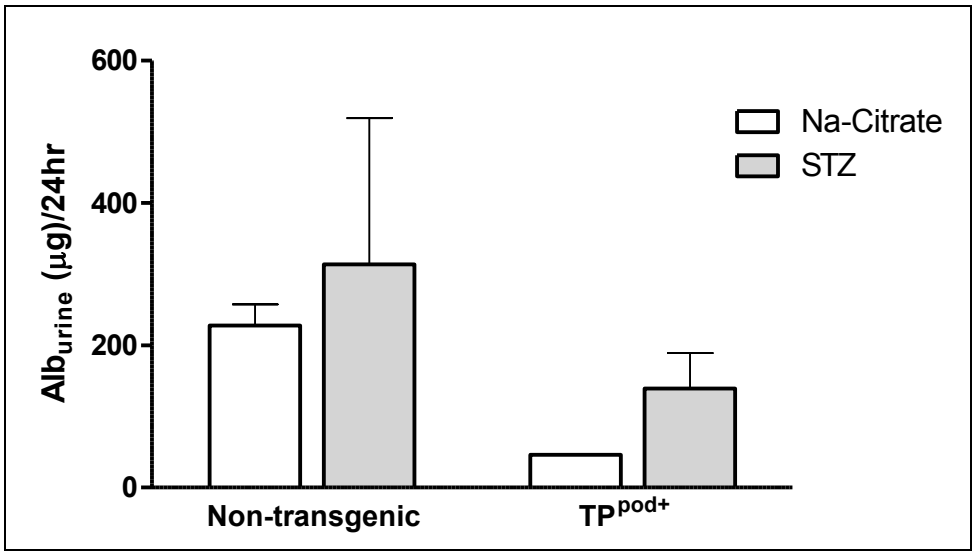

Figure 34: Mild glomerular filtration barrier damages in low dose STZ mice.

24 hour urine collection samples were submitted to albumin quantification using the Mouse Albumin ELISA Kit (Bethyl Laboratories Inc.) and have been normalized to 24 hour volume. Both non-transgenic and TP^{pod+} STZ-injected mice have a higher level of albuminuria (314 ± 206µg/24hrs [*n*=4] and 139 ± 50µg/24hrs [*n*=3], respectively) than their non-diabetic controls (228 ± 30µg/24hrs [*n*=2] and 46µg/24hrs [*n*=1], respectively). Due to the little number of samples, the two-way ANOVA statistical analysis done in GraphPad Prism, was unable to detect a difference between either group.